11/30/2021

Prosthetic design for ankle-foot stiffness and angle for persons with transtibial amputations

Ph.D. Preliminary Exam

Mechanical Engineering

Preliminary examination committee

Peter Adamczyk, Ph.D.

Darryl Thelen, Ph.D.

Katherine Fu, Ph.D.

Aaron Dingle, Ph.D.

Justin Williams, Ph.D.

Kieran Nichols, M.S.

BADGER LAB

ABSTRACT

Persons with unilateral transtibial amputations lose the biological ankle and foot. To regain functional walking, they utilize ankle-foot prostheses. These prostheses can vary in cost and complexity depending on their adaptability, weight, and comfort. The simplest and cheapest designs exist as passive mechanical prostheses, and the most complex and expensive designs are from active robotic prostheses. In between these two extremes of passive and active prostheses, semi-active prostheses allow users to modulate mechanical functions with simpler design, lower cost, and less power than active prostheses. In addition, they could replicate more of the biological ankle-foot functions than passive prostheses.

The background for this dissertation explored the main principles of prosthetic design, prosthetic-walking mechanics, and sensor feedback. Many users adapt their walking with passive transtibial prostheses with biomechanical gait deviations like hip circumduction, toe scuffing, weak prosthetic side push-off, hyperextension on the prosthetic side, and higher intact-side collision energy. Knee osteoarthritis on the intact side may become an eventual consequence of those gait deviations. Current semi-active prosthetics attempt to minimize those gait deviations with improved design and sensor feedback. This Preliminary document presents the biomechanical evaluation of a Variable Stiffness Foot (VSF) and proposes a future investigation of the design and biomechanical evaluation of a Two-Axis aDaptable Ankle (TADA). These two prostheses were chosen to give users modulation of the essential ankle-foot functions of stiffness and ankle angle.

The Past work of this dissertation focused on the VSF, which can modulate foot stiffness during the swing phase of the prosthetic limb. Persons with transtibial amputations walked across two force plates in a motion capture lab. A stiffer VSF was associated with peak magnitude changes of decreased ankle dorsiflexion angle, increased ankle plantarflexor moment, increased knee extension, decreased knee flexor moment, and decreased prosthetic energy storage, energy return, and power. This work fed into developing a computational contact VSF model used by external collaborators, which predicted the resultant and center of pressure of the ground reaction force under the prosthesis. Additionally, a Variable Stiffness Foot with Two Keels (VSF2K) was designed to allow both hindfoot and forefoot stiffness modulation for future research.

The Current and Future work of this dissertation will focus on the TADA, which can modulate ankle angle during the swing phase of the prosthetic limb. The TADA is an adaptable two-axis ankle modulated by two motors with encoders and hall sensors, an inertial measurement unit, and a load cell. The first aim will focus on the mechanical validation of the TADA control system. This system will be validated with non-disabled persons to test for correct ankle angles and ankle moment detection. In the second aim, the TADA system will be evaluated during out-of-lab walking in persons with transtibial amputations. The biomechanical effects of three control laws for the TADA will be evaluated. They consist of lifting the toe during every swing phase, anticipatory slope-matching control (matching the ankle angle with the floor angle), and moment-limiting control (lowering the mean ankle moment to a target ankle moment). The tests will compare the effects of these different adaptable control options of the TADA with the fixed neutral TADA angle.

Table of Contents

Chapter 1. BACKGROUND 1

(a) Introduction 1

(b) Main Principles of Prosthetic Design 1

(c) Prosthetic Sagittal Mechanics in walking 5

(d) Prosthetic frontal mechanics in walking 10

(e) Lower limb sensor feedback in prosthetic walking 15

(f) Gaps and research opportunities 18

Chapter 2. PAST WORK 20

(a) Introduction 20

(b) Variable Stiffness Foot (VSF) Description 20

(c) Sensitivity of Joint Mechanics to Various Forefoot Stiffnesses of the Variable Stiffness Foot (VSF) in level-ground walking 21

(d) Published Collaboration Manuscripts 33

(e) Development of VSF with hind and forefoot properties 35

(f) Conclusion 36

Chapter 3. CURRENT AND FUTURE WORK 37

(a) Objective of Current and future work 37

(b) TADA description 37

(c) Specific Aims 39

(d) Methods 41

(e) Conclusion 45

(f) Impact of Proposed Work 45

Chapter 4. TIMELINE 47

(a) Past work (Pre-2021) 47

(a) Current and Future Work (Jan 2021 - May 2023) 47

(b) End of Ph.D. (June 2023 - Dec 2023) 48

Chapter 5. NOMENCLATURE 49

Chapter 6. LISTS OF FIGURES AND TABLES 50

(a) List of Figures 50

(b) List of Tables 50

Chapter 7. REFERENCES 51

Chapter 1. BACKGROUND

(a) Introduction

People with lower-limb amputations account for about one million people in the United States of America, with about 28% being individuals with transtibial amputation (TTA)[1,2]. Besides the high average cost of about $81,000 for TTA amputation and associated rehabilitation services[3], prosthetic users spend about $1600 per year for a prosthetic device that lasts on average 1.3 years[4]. The primary function of these lower limb prostheses is to regain walking on level ground but are also necessary for standing, walking on stairs and ramps, and uneven terrain. These prosthetic devices attempt to return walking functionality by mimicking some aspects of the human ankle-foot mechanics that were lost. This attempt to return to walking for these persons with unilateral transtibial amputations is difficult as the necessary walking mechanics are not fully understood. The problems of high cost and difficulty in recreating the human ankle-foot system instigate a need for improved mechanical adaptabilities and characteristics of the prostheses.

(b) Main Principles of Prosthetic Design

(i) Common characteristics of prosthetic walking

To mechanically connect to a person with TTA, the prosthetic foot-ankle device has an attachment area on its residual limb via a socket-suspension interface. This interface allows the prosthetic lower limb to be attached to the residual limb, which distributes the loading forces through a liner and its many contact points on the remaining part of the residual limb. The socket-suspension interface connects to a pylon adaptor that allows height adjustability. The pylon adaptor then connects to the prosthetic device.

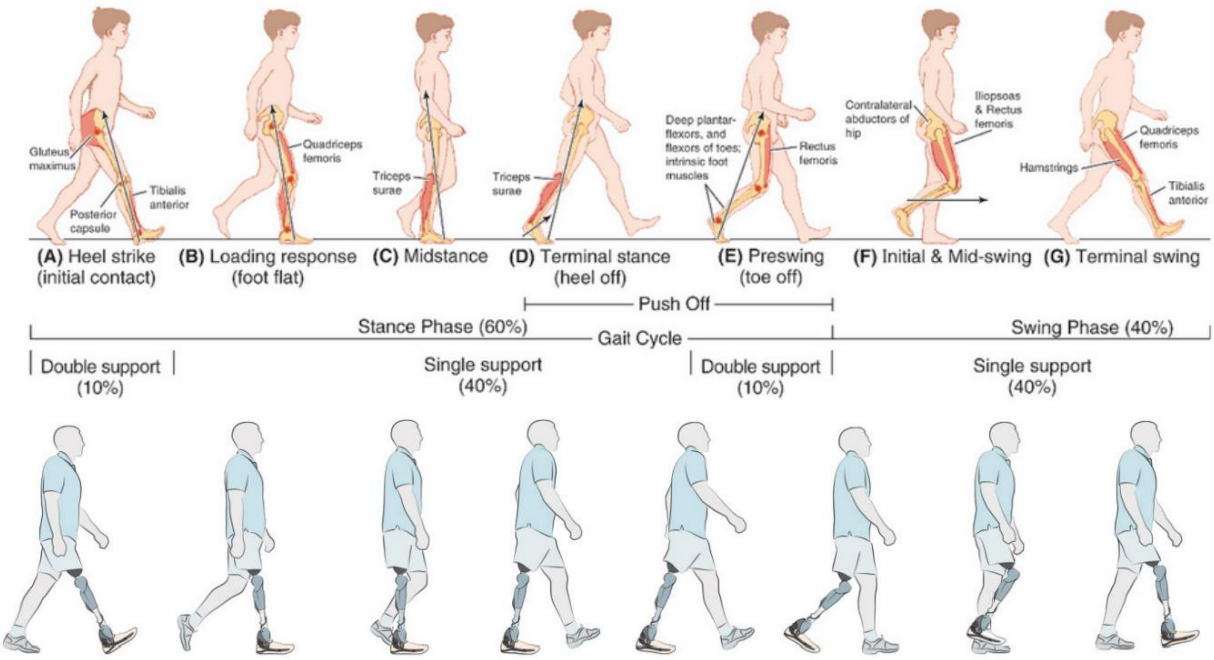

Figure 1: graphical representation of gait events of a non-disabled person and person with a prosthetic leg from Rajukova et al.[7]

Human walking (see figure 1) involves a periodic cycle where the two legs move the body forward in two phases: stance (about 60% of the cycle) and swing (about 40% of the cycle)[5]. During the swing, only one leg is in contact with the ground, and one or two legs are in contact with the ground during stance. Typically, the foot first contacts the ground with a heel strike, transitions to foot flat, heel off, and ends with toe-off. Non-disabled humans (no amputations) depend on their multiple leg muscles that cross the hip, knee, or ankle joints to modulate the joint position and moment to apply the appropriate ground reaction forces.

The hip, knee, and ankle mechanics' nomenclature will be introduced in the following sentences. Mechanically, hip motion is described by hip flexion and extension with moments of hip flexor and extensor. Knee motion is described by knee flexion and extension with moments of knee flexor and extensor. Ankle motion is described by ankle dorsiflexion and plantarflexion with moments of ankle dorsiflexor and plantarflexor[6] (see figure 2). A person with a transtibial amputation typically relies on an ankle-foot prosthesis (transtibial prosthesis) to walk. They have lost the original functionality of the ankle-foot system and must rely on the replacement passive or powered ankle-foot prosthesis.

Persons with transtibial amputations have many biomechanical issues, which they must compensate for by adjusting their gait. Issues[7] include vaulting where the person steps up with their intact side to complete the prosthetic side swing, circumduction consisting of the prosthetic foot swinging outward during the swing phase, hyperextension (locking) of the knee on the prosthetic side, and lateral trunk bending consisting of the person having a forward-leaning torso during prosthetic side stance. These issues could be caused by improper fitting and alignment and be reduced by a more suitable prosthesis. Prosthesis research aims to improve prosthesis design and fitting to minimize the need for these compensations.

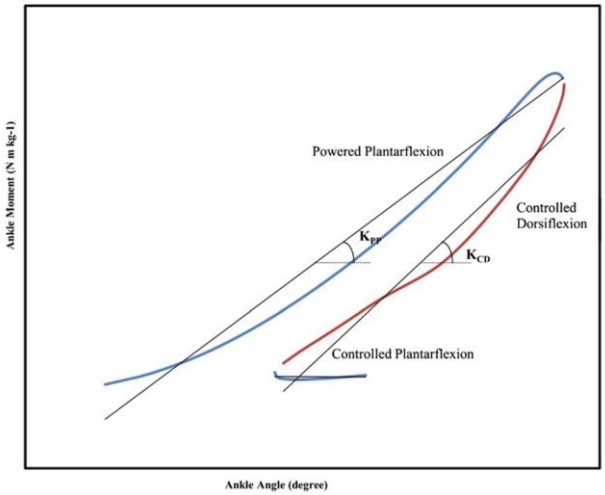

Figure 2: Non-disabled ankle moment vs. angle of the stance phase of typical walking from Safaeepour et al.6 Stance phase starts with controlled plantarflexion, transitions to controlled dorsiflexion, and ends with powered plantarflexion. Stiffness relates to the slope of ankle moment and angle.

(ii) Design of Lower Limb Prostheses

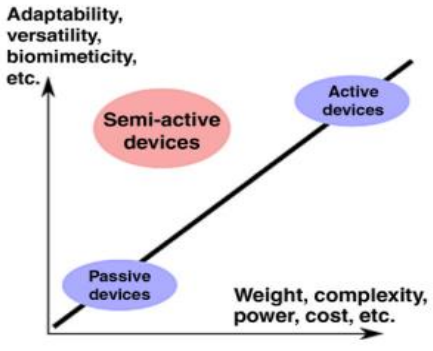

Figure 3: Various considerations in developing passive, active, and semi-active prostheses from Adamczyk[8]

The main aim of the prosthetic design is to allow the users to have a functional gait when interacting with the prosthetic device. Prosthetic devices restore standing, walking, and running locomotion, giving users mobile self-sufficiency instead of using crutches or a wheelchair. Prostheses can be categorized in terms of adaptability into three main groups: passive, semi-active, and active (see figure 3). Passive prostheses which have static mechanical properties are more widely accessible and affordable. On the other side of the adaptability spectrum (see figure 3), active (robotized) prostheses offer users an extensive range of biomimetic functions, including modulation of posture, impedance, and

power. Still, their disadvantages stem from their weight, increased size, expensive, high energy demand, and control complexity[8].

Energy Storage and Return (ESR) prostheses are useful passive prostheses that offer some passive adaptability and returned functionality to persons with transtibial amputations. ESR prostheses absorb mechanical energy using viscoelastic deformation in early-to-mid-stance and return it during mid-to-late stance. In addition, ESR prostheses offer biological ankle-foot functions like impact absorption, gradual center of pressure advancement, and some push-off energy due to viscoelastic recoil[9,10,11]. To assess the usefulness of the ESR prostheses, one proposal[12] created standardized tests to establish essential features to evaluate prosthetic feet for prescription, including pylon, heel, and axis tests. Another report[13] put forward that ankle-foot prostheses can be differentiated by two main factors: normal stiffness (superior-inferior direction to foot) and foot geometry/alignment, which includes ankle angle. Ankle-foot stiffness and foot geometry/alignment are essential for passive prosthesis design as they affect all parts of prosthetic gait. For example, higher foot stiffness is associated with lower push-off work and gait asymmetry during late stance[9,] and an overly long foot is associated with more toe scuffing during the swing phase[14].

In between the adaptability extremes of passive and active prostheses exist the semi-active prostheses. Semi-active prostheses allow some modulation of mechanical properties but cannot supply positive energy during the stance phase. Their mechanical properties[8] range from exploiting the gait cycle by changing swing phase ankle angle where ankle loads are low, combining non-backdrivability and high static forces by benefiting from friction on an inclined plane, and using springs to replace motors by using a spring-loaded ankle mechanism to match ankle angle according to the slope of the ground. Though positive energy is not supplied during stance, these prostheses can allow users more adaptability at a fraction of the cost, weight, and sometimes complexity. Adamczyk[8] proposed essential questions to ask when designing an appropriate prosthetic foot-ankle device to be, “How could a semi-active device accomplish the goal, and how and when should the prosthesis adapt?” To evaluate the prosthesis

performance, they proposed that we ask: “Does it work, does it have the intended effect, and do people like it.”

Three prominent types of semi-active mechanisms are hydraulic devices, adaptable stiffness, and ankle angle control. Hydraulic prostheses use pressurized fluid to dampen joint motion. Several ankle-foot systems[8] use variable hydraulic dampers like Endolite *Elan*[15], Freedom Innovations *Kinnex*[16], and the Ottobock *Meridium*[17]. Adaptable stiffness prostheses like the *Variable Stiffness Foot* and *Variable Stiffness Prosthetic Ankle* change ankle-foot stiffness to affect ankle and knee mechanics. The Ossur *Proprio* foot[18] changes the ankle angle in swing phase under active control[8,18].

To further understand how to create main principles for ankle-foot prosthetic design, we must describe the observable walking mechanics common in walking for persons using transtibial prostheses.

(c) Prosthetic Sagittal Mechanics in walking

Firstly, much of walking mechanics focuses on sagittal kinematics and kinetics as walking moves along the anterior-posterior (sagittal) axis (forward direction of walking). The sagittal plane breaks the body into right and left with its perpendicular axis predominantly describing flexion/extension. Its dimensions are vertical and anterior-posteriorly horizontal. The lower-leg prostheses primarily affect the hip, knee, and ankle joints and their relevant upper-leg, lower-leg, and foot segments. Also, summative mechanics like the center of mass work and acceleration give valuable information for describing the effect of lower leg prosthetics on walking. This section will describe the prosthetic sagittal walking mechanics by starting with the ankle-foot system, then knee mechanics and hip, and ending with the center of mass (COM) summative metrics.

(i) Ankle-foot mechanics

Adamczyk[8] proposed three different concepts of ankle-foot functions: Foot roll-over where the center of pressure (COP) as a function of the lower leg angle can be related with the instantaneous effective radius of the ankle-foot; angular stiffness where ankle moment is related to ankle angle like a lever mounted to a torsional spring; ankle angle control where the neutral ankle angle or set point by

which the spring/shape like behavior is relative to that neutral angle. These ankle-foot concepts are different ways to model ankle-foot behavior.

Raschke et al.[19] found that persons with TTA preferred less stiff feet while walking, associated with 15% lower peak sagittal prosthetic socket moments. Furthermore, Fey[20] offered that decreased foot stiffness leads to increased prosthetic ankle range of motion, mid-stance energy storage, and late stance energy return. Also, Klodd et al.[10] reported that dorsiflexion angle and ankle plantarflexor moments increased with a stiffer forefoot. To further explore the effect of foot stiffness on walking mechanics, Adamczyk et al.[9] examined the hind/forefoot stiffness effects on prosthetic walking for different stiffnesses and walking speeds. In general, they found that a stiffer hindfoot yields decreased prosthesis energy return, larger vertical ground reaction force (GRF) loading rate, larger knee flexion angle (stance phase), and knee extensor moment. They also found that a stiffer forefoot yielded decreased prosthetic ankle and COM push-off work and larger knee extension angle and knee flexor moment in late stance.

Glanzer and Adamczyk[21] created a Variable Stiffness Foot (VSF) as an adaptable stiffness prosthetic foot. It offers a semi-active modulation of its forefoot stiffness during the swing phase. The VSF has a rigid ankle, and its forefoot acts as an overhung beam that can modulate the forefoot stiffness by adjusting a support fulcrum to change the overhang length. They reported that VSF users displayed greater energy storage and return with lower stiffnesses.

As another stiffness-based prosthesis, the Variable Stiffness Prosthetic Ankle (VSPA)[22] utilizes a cam-based transmission to allow selectable nonlinear ankle torque-angle curves and modulate forefoot stiffness through motorized leaf spring configurations. VSPA allows the users to set their ankle and foot stiffnesses according to their preferences and mobility tasks. Gait testing with VSPA resulted in increased peak plantarflexor moment and increased peak dorsiflexion angle with increased stiffness. Quraishi et al.[23] further adapted the VSPA to have decoupled energy storage and return where energy was stored at heel strike and during loading and returned later in the gait cycle. These mechanics can also allow suitable ankle changes for toe clearance and increased push-off power during the swing phase.

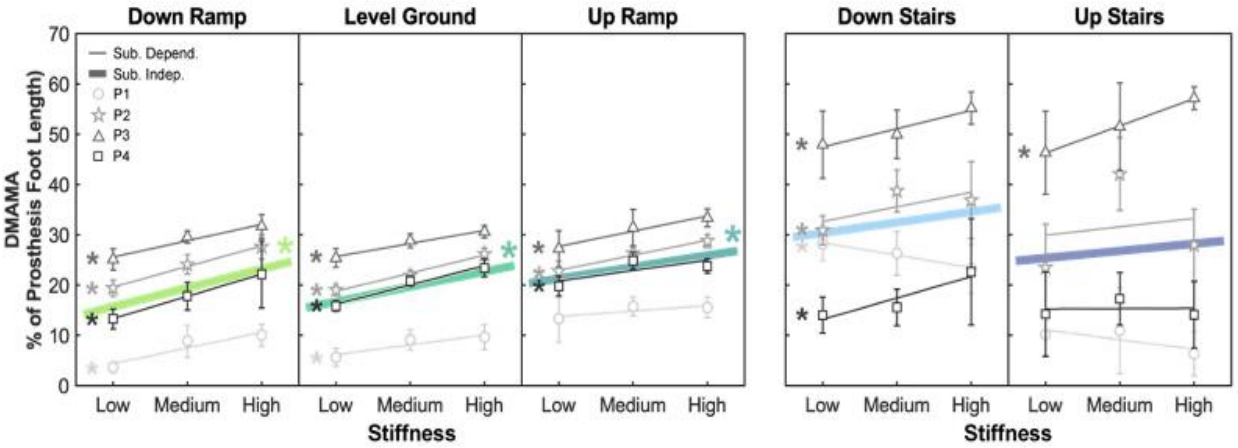

Figure 4: linear mixed model trends showing the relationships of prosthetic forefoot stiffness on DMAMA for various locomotion modes from Leestma et al.[18] The persons with transtibial amputations walked on level ground, up and down ramps, and up and downstairs. Color lines represent the subject-independent linear mixed effect regressions. Gray markers, vertical bars, and lines show each person's average, standard deviation, and subject-specific linear fit. The asterisk (*) represents a significant linear trend (p-value < 0.05).

Effective control of the stiffness modulation in walking and running can be connected to the Dynamic Mean Ankle Moment Arm (DMAMA)[24]. DMAMA represents the ratio of sagittal ankle moment impulse to vertical ground reaction force impulse during the stance phase of gait. Adamczyk[24] results showed that GRFs move closer to the ankle (less forward) with increased walking speed in natural gait. As a follow-up, Leestma et al. [18] analyzed persons with transtibial amputations walking on level ground, ramps, and stairs. They found a positive linear sensitivity of DMAMA (more forefoot dominated) to stiffness and ground incline while walking with the VSF (see figure 4). This metric, DMAMA, could be used as a control loop variable to adapt semi-active prostheses to various locomotion modes like

standing and walking on level, ramps, and stairs. In addition, DMAMA could also evaluate the biomimetic performance of various passive and active prostheses.

Persons with ankle-foot prostheses have poor proprioception in their lower leg due to the transtibial amputation. As they interact with these prostheses, they use their residual limbs to perceive the prosthetic ankle-foot mechanics. Shepherd et al.[26] added that persons with TTA can repeatably select their preferred stiffness within a mean coefficient of variation of 14.2% and could identify a 7.7% change in ankle stiffness with a 75% accuracy. Along with stiffness, individuals also can perceive ankle damping. For example, Azocar et al.[27] reported that persons with amputations could perceive damping changes of at least 12.0% at the ankle and highlighted those persons with amputations could perceive changes of at least 11.6% and 13% for ankle and knee stiffness, respectively.

(ii) Knee and hip mechanics

The prosthetic ankle-foot directly affects a prosthetic user's ability to modulate their ankle torque and angle. These ankle mechanics also influence more proximal joints like the knee and hip. Ankle mechanics have dominant contributions to the center of pressure excursion, push-off power, and energy storage and release. In contrast, knee and hip mechanics heavily contribute to body support during the stance phase and swinging the leg without floor contact during the swing phase. Common knee and hip issues with persons with TTA are hyperextended (locked) knees during stance phase, toe scuffing, and more hip effort during swing phase.

Ingraham et al.[28] proposed that even though excess prosthetic ankle work (more than biological values) has been thought to help reduce hip effort compensations, it may be a diminishing negative return. In the intact leg, the bi-articular (knee and ankle) gastrocnemius muscle help reduce excessive knee extension during stance. However, in a prosthetic foot-ankle that does not have that bi-articular restraint, excessive ankle plantarflexor moment is associated with knee hyperextension[13,21].

Wu et al.[30] explored the determinants of ground foot clearance during leg swing and found that foot movement is not only determined by the separate costs of lifting the foot high (positive foot clearance) or scuffing your foot on the ground (negative foot clearance). They found that the cost for scuffing increased twice as steeply as that for lifting (see figure 5) and indicated that it might also be due to movement variability, which influences the average cost of walking.

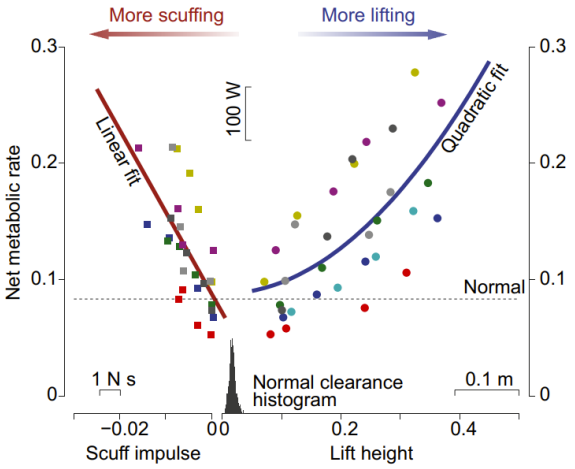

Figure 5: Net metabolic rate as a function of measured scuff impulse and toe lift height from Wu et al.[24] The toe clearance height and scuff impulse were normally distributed, meaning that more of the scuffs had low magnitude scuffs and low lift height.

To investigate energy storage and return in walking, Adamczyk et al.[31] found that push-off impairment and its related compensations are related to some asymmetries in walking for people with unilateral transtibial amputations. Lower prosthetic energy return leads to lower push-off work by the impaired limb, leading to greater energy loss in the intact leg/ground collision. Prosthesis users may compensate by adding positive hip work during the intact leg or prosthetic leg stance phase. That compensation was observed with a semi-active energy-recycling prosthesis, the controlled energy storage, and return (CESR) prosthesis[32]. Segal et al.[33] showed that using CESR with low stiffness increased prosthetic push-off (energy return) and decreased intact limb COM collision work compared to using a conventional foot.

(iii) Whole-body metrics: center of mass

Beyond the prosthetic energy flow, whole body metrics like energy expenditure and center of mass mechanics (COM) also need to be discussed. Zelik and Adamczyk[34] showed a unified effect of ankle energy return that contributes to both leg swing and COM acceleration in able-bodied walking. Zelik et al.[35] found that lower prosthetic foot stiffnesses led to higher energy storage, energy return, and prosthetic limb center of mass (COM) push-off work. Walking energy expenditure in their participants with TTA was lowest for intermediate stiffness. This statement agreed with Klodd et al.'s suggestion[10] that there might be biomechanical disadvantages to the lowest stiffness despite higher energy return. One biomechanical disadvantage involved the "drop-off" effect in late stance, which is reduced ankle plantarflexor moment that allows the COM to "drop off" the end of the foot during load transfer from the prosthetic side to the intact side[10]. The persons with TTA from Zelik et al.[28] showed higher hip work with lower energy transfer from the prosthesis to the COM, which could be attributed to higher energy dissipation at the knee. Spring compliance (inverse of stiffness) influences push-off but has co-occurring biomechanical trade-offs limiting how push-off can benefit the walking economy (lower metabolic cost). Additionally, Clites et al.[36] agreed that subject-preferred stiffness had no correlation with energy expenditure, but it also found that stiffness tended to be lower for self-selected speed.

(iv) Summary

The distinctive features of sagittal prosthetic mechanics include sagittal ankle, knee, and hip angles, work, and moments, push-off energy and energy storage, vertical ground reaction force, DMAMA, and foot clearance.

(d) Prosthetic frontal mechanics in walking

Along with sagittal plane compensations, people with transtibial amputations also have distinctive frontal (coronal) plane issues. The frontal plane divides the body into front and back. Common descriptors of frontal plane motion are inversion/eversion and adduction/abduction. Moments are described as invertor/evertor and adductor/abductor.

(i) Ankle-foot mechanics

Kim et al.[37] performed a test with an ankle-foot prosthesis emulator that modulated inversion/eversion moments using stiffness trajectories and found that positive ankle inversion stiffness could lower the active control requirements compared to zero stiffness conditions in flat ground walking. They alluded to active control being managed by foot placement variability[38], margin of stability[39], and intact limb center of pressure control[40]. Additionally, Velzen et al.[41] found that the systematic effects of prosthetic misalignment were evident in horizontal magnitude and moment arm from the ankle of the frontal ground reaction force (GRF) during late prosthetic stance. They showed that the magnitude of the mediolateral horizontal GRF was significantly less with an internally rotated prosthesis (inward rotation of knee along the tibial long axis), compared to knee adduction (knocked knees) and externally rotation (outward rotation of knee along the tibial's long axis). Also, the moment arm was more lateral when the prosthesis was externally rotated.

van Hal et al.[32] demonstrated that mediolateral balance is dominated by hip frontal moments and that passive mechanical stability is dependent on the curvature of the loaded prosthetic foot. In addition, they investigated the prosthetic roll-over curvatures and found that a limiting factor for applying frontal moments is the lagging (hysteresis) of the center of pressure displacement due to material compliance and slip of the shoe, which suggests that shoe design to prevent these issues is essential to consider.
Segal and Klute[43,44] found that recovery strategies differ minimally between stiff and compliant prosthetic feet. They suggested that prosthetic mediolateral compliance is less necessary, and hip frontal moments during the stance phase may be necessary.

Ramstrand and Nilsson[45] showed no significant difference in stair walking between persons with amputations and non-disabled individuals in foot placement (foot entirely on the stair) and foot clearance. However, for stair ascent and descent, the persons with amputations walked with a slower velocity and cadence, increased stance phase and double support time, and increased their step width compared to the non-disabled individuals.

(ii) Knee/Hip mechanics

Boone et al.[36] investigated the perturbation effects of TTA prosthetic misalignment on the sagittal and frontal (coronal) socket reaction moments. These prostheses had misalignment perturbations of 3 and 6 deg rotation (adduction/abduction) and 5 and 10 mm translations (medial and lateral). Compared to normal alignment, frontal socket moments had the most statistically significant differences at 30% and 75% of the stance phase for all angles and translation perturbations (see figure 6). Royer and Wasilewski[47] demonstrated that persons with unilateral transtibial amputations had 46% and 39% higher peak knee and hip internal abduction moments on the intact side compared to the prosthetic side. The participants also had 17% and 6% higher peak knee and hip external abduction moments on the intact side compared to the prosthetic side. These results suggest higher joint loading on the intact side, which may predispose the participants to premature joint degeneration like knee osteoarthritis.

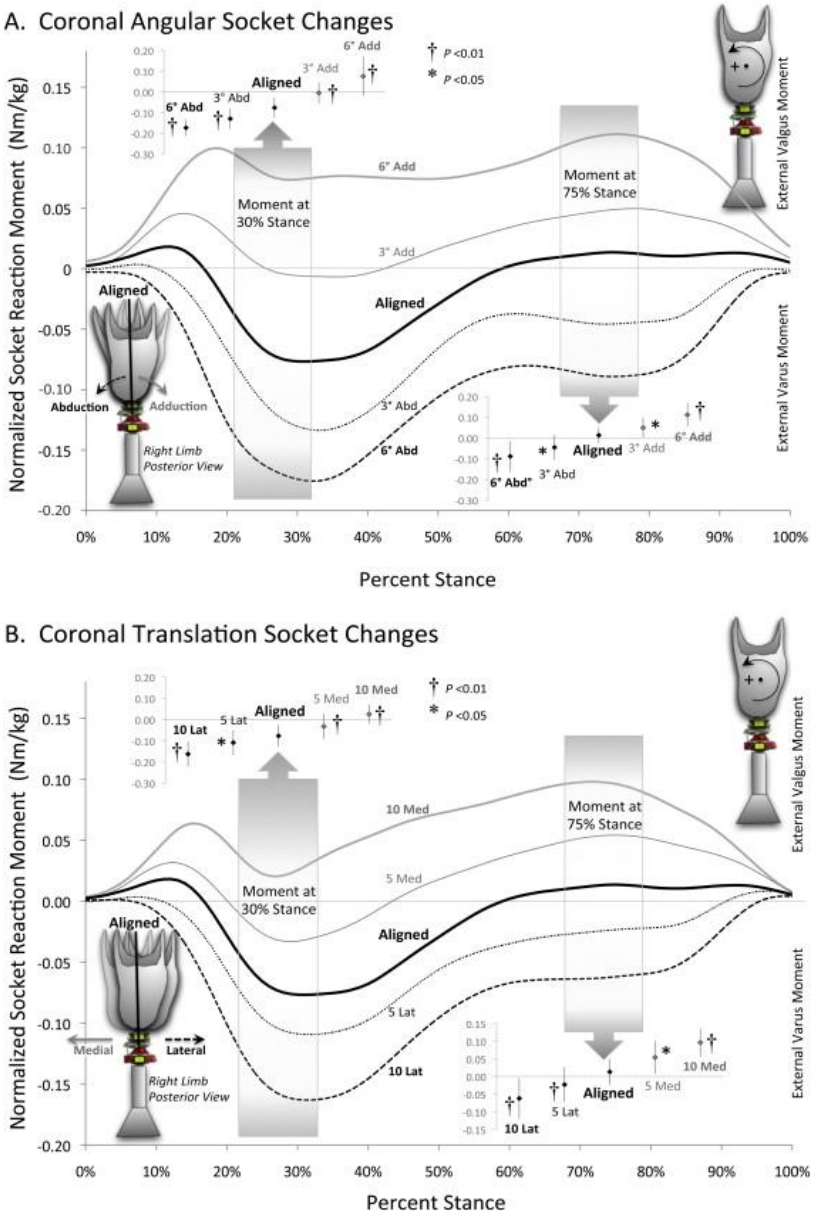

Figure 6: Normalized socket reaction moment in response to frontal (coronal) angular and translational socket changes from Boone et al.[36] The frontal socket reaction moments were shown for angular perturbations (Graph A) and translational perturbations (Graph B).

Morgenroth [48] investigated the potential contributors to knee osteoarthritis in persons with lower-limb amputations (see figure 7). They found a negative correlation of higher prosthetic push-off with lower first peaks of intact knee external adduction moments (KEAM). Jin et el[49] added that higher first peaks of KEAM and higher loading rates were also associated with using higher damped prosthetic feet vs. lower damped ones. When looking at sloped walking, Doyle et al.[50] showed that the first peak of KEAM and the rate at which KEAM increased (KEAM loading) were the only significant results where downhill had the largest KEAM loading compared to flat, uphill, and right and left cross slopes.

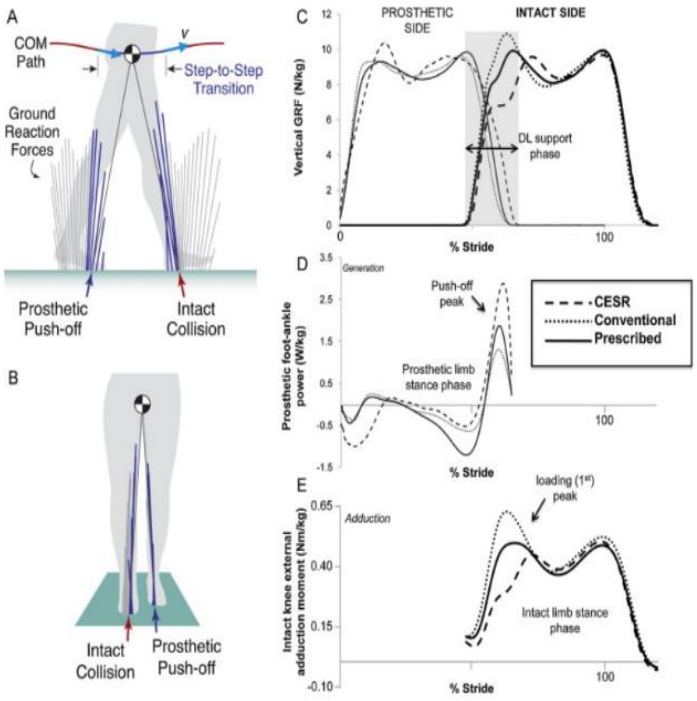

Figure 7: sagittal and frontal representations (A and B) of prosthetic and intact side collision and push-off. Graphs of vertical GRF (C), prosthetic foot-ankle power (D), and intact knee external adduction moment (E) vs. percentage of stride were shown from Morgenroth et al.[41]

Rueda et al.[51–53] showed that participants with TTA walked with less hip abductor and valgus (knee) moments on the prosthetic side compared to the intact side and the non-disabled subjects. They also found that the thorax frontal range of motion increased, indicating mediolateral compensation to accommodate the prosthetic vs. intact frontal moments. Ventura et al.[54] showed that subjects who walked along a circular path primarily relied on larger sagittal hip joint work to turn compared to persons with no amputations who relied on more sagittal ankle work with the residual leg in and outside of the turn. Additionally, Segal et al.[33] found that persons with TTA have decreased prosthetic mediolateral ground reaction impulse and stride length suggesting a more centered COM over the base of support, which may lower the risk of falling.

(iii) Whole-body metrics: center of mass and angular momentum

A useful measure of dynamic walking stability is the margin of stability (MOS), which incorporates the relationship of COM movement and foot placement in the person staying upright while walking[55]. The margin of stability is the mediolateral distance between the edge of a person's base of support and the velocity-adjusted (extrapolated) position of the center of mass at an instant of time. Gates et al.[39] found that persons with TTA who walked on a loose rock surface had larger average minimum margins of stability (min MOS) than their non-disabled participants. In addition, persons with TTA had decreased min MOS on their prosthetic limb compared to the intact limb. Overall, these non-disabled people and persons with TTA had increased step width mean and variability, COM range of motion, and peak COM velocity when walking on a rocky surface. Interestingly, the persons with TTA had higher variability of step width and min MOS, which may indicate that they are making larger step-to-step corrections to achieve the same average result.

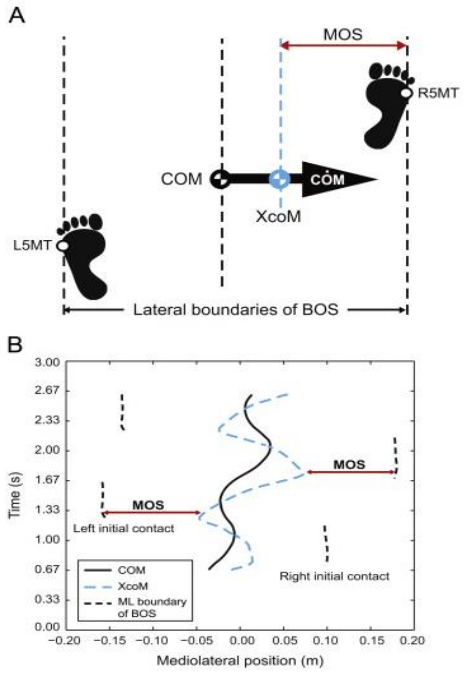

Figure 8: conceptual diagram (A) and numerical graph (B) showing the relationship of the center of mass (COM) mediolateral position, extrapolated COM (xCOM), base of support (BOS), and margin of stability (MOS) from Beltran et al.[46]

Beltran et al.[56] tested persons with TTA and non-disabled individuals on walking trials on the Computer Assisted Rehabilitation eNvironment (CAREN). The conditions involve no perturbations and pseudo-random mediolateral translations of the visual field and platform (see figure 8 for MOS representation). Persons with TTA had a larger mean and variance of the MOS in the platform oscillations compared to the non-disabled walkers, but not the visual oscillations, which the authors attributed was due to people with TTA having a lack of active ankle control and ankle proprioception. [57]

In Miller's Master's thesis[58], they looked at the balance recovery mechanisms of persons with TTA following

mediolateral translational perturbations using a pneumatic device attached to the ankle. They found that participants had decreased range of frontal angular momentum and increased hip joint work for lateral perturbations and decreased hip joint work and increased range of frontal angular momentum for medial perturbations. Shell et al.[59] investigated the mechanical effects of decreased frontal stiffness of the prosthetic ankle with persons with TTA walking on a circular path. When their residual limb was on the inside of a 1m circular turn, the frontal hip work increased, decreased residual and increased intact limb vertical ground reaction impulses, and the frontal range of whole-body angular momentum decreased.

(iv) Summary

The distinctive features of prosthetic frontal mechanics include frontal ankle, knee, and hip moments and work, step width, mediolateral and vertical ground reaction force, margin of stability, and frontal angular momentum.

(e) Lower limb sensor feedback in prosthetic walking

(i) Identifying prosthetic state

There are many ways of identifying the spatiotemporal properties of a person wearing a prosthetic lower limb. Several measurements systems that are utilized contain force or pressure plates, optoelectronic, wearable motion capture devices (inertial measurement units), and smart clothes. In the laboratory, one of the most common methods utilizes the motion capture system with infrared cameras (optoelectronic) and reflective markers, and force plates. This method yields high precision and intra-trial repeatability but lacks portability, and its results are sensitive to setup. A methodology that has become more popular[5,60] and helps determine the human body's kinematics (translational and rotational position, velocity, and acceleration) is the use of Inertial Measurement Units (IMUs). To add further information about the interaction of the prosthetic device with the environment, load cells[5] can be used to identify the kinetic interaction (translational and rotational forces and moments).

(ii) Kinematic and kinetic sensing of gait events

Many currently produced IMUs contain gyroscopes, accelerometers, and magnetometers that measure rotational velocity, translational acceleration, and earth's magnetic North (to help with integration drift). Several IMU-based methods[5] have been used to identify gait events like heel contact and toe-off with IMUs attached to the foot, pelvis, or shank. When combined with portable force sensors like load cell or foot pressure soles, the gait detection algorithms[5] improved the robustness of identifying transitions between gait events (stance to swing) and sub-phase events of stance and swing.

Washabaugh et al.[61] showed that IMUs had moderate to high validity of spatiotemporal gait parameters in healthy young adults among multiple days of walking speeds and were repeatable on treadmill and overground walking. In addition, they found that motion reconstruction, which depended on foot IMUs, gave better gait parameters than placing the IMU at the ankle.

Li et al.[62] developed and tested a walking speed estimator that used a shank-mounted IMU (gyroscope and accelerometer) with relatively high accuracy (under 5% error) for various treadmill speeds and slopes. The estimator was statically calibrated to determine the gravity axis and modeled the shank's movement like an inverted pendulum. This model sets the horizontal velocity of the IMU to zero when the shank is vertical (around mid-stance).

Rebula et al.[63] demonstrated that a foot-mounted IMU could be used to estimate mean stride lengths and duration within 1% of motion capture. They displayed the success of motion reconstruction using the zero-velocity property when the foot is flat on the ground (referred to as a zero-velocity update). Also, they offered the algorithm steps for motion reconstruction of step segmentation, rotational orientation estimation, translational velocity estimation, and trajectory formation (see figure 9 on the following page). Kitagawa et al.[64] added foot clearance calculations as an output to the previous motion

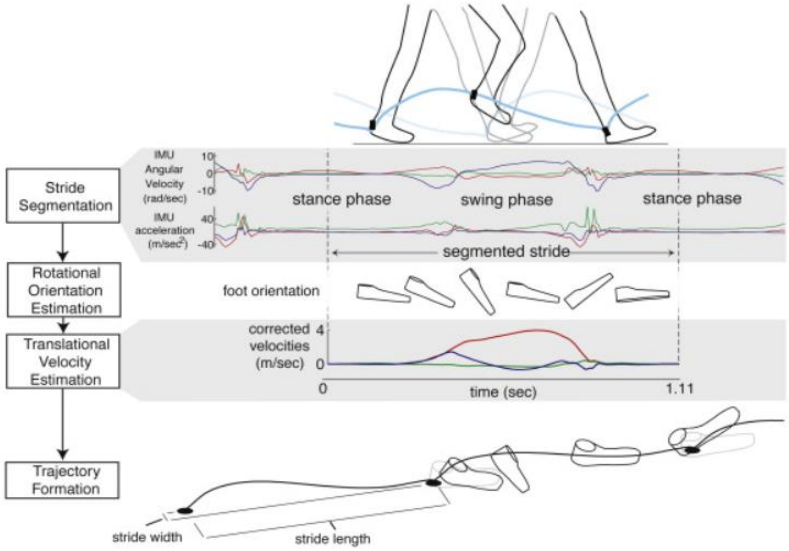

Figure 9: Motion reconstruction steps with representative data trajectories from Rebula et al.[57]

reconstruction method. They used a foot IMU with an adjusted zero vertical displacement assumption across multiple strides. They found that mean accuracy and precision for foot clearance were 2±7 mm. Previous researchers[64,65] have defined foot clearance during the swing phase as the vertical displacement of the foot IMU from the floor. The minimum foot clearance (MTC) is associated with tripping and falling if the value is too low[30].

(iii) Locomotion modes

Previous work[66] has shown the validity of locomotion mode classification in transtibial prostheses discerning between level-ground walking, stair ascending, stair descending, ramp ascending, and ramp descending. They used two IMUs (shank and foot), where the studies had more than a 95% recognition accuracy for each locomotion mode. Sup et al.[67] showed that two slope angles (5 and 10 degrees) were detected and estimated in knee/ankle prosthetic walking. They used a three-axis accelerometer attached axially along the prosthetic shank and two load cells (one under heel and another under ball of foot) to detect when the prosthetic foot is parallel with the ground.

(iv) Feedback in lower limb prosthetic walking

Feedback in prosthetic gait is essential to help the users achieve functional gait. Ankle-foot stiffness and ankle angle have commonly been used as the feedback variable to adjust gait mechanics. Clites et al.[36] found that participants with transtibial amputations preferred lower ankle stiffness at self-selected treadmill walking speeds and the same/higher stiffness for faster self-selected overground

walking. These preferred stiffnesses were associated with kinematic symmetry between prosthetic and intact joints but not with body mass or metabolic rate.

Best et al.[68] presented a phase variable controller for a powered knee-ankle prosthesis that adjusted knee and ankle mechanics depending on various speeds and inclines. They developed a task estimator with a joint position controller, and it identifies steady gait, speed estimation, incline estimation. Their closed-loop controller contained a knee and ankle actuator, one IMU on the thigh, and a load cell at the ankle. It was robust to discontinuous task changes and converged in less than five steps to the specified target.

(v) Summary

The key uses of lower limb sensor feedback in prosthetic walking include: using inertial measurement units and load cells to detect prosthetic state; estimating gait events like heel strike, toe-off, and leg swing; reconstructing prosthetic movement, ground reaction forces, and joint moments; classifying if the gait is over flat or sloped ground; and finally using the prosthetic sensor feedback to adjust ankle-foot stiffness and angle.

(f) Gaps and research opportunities

Persons with unilateral transtibial amputations need appropriate ankle-foot prostheses for walking. They have typical gait deviations and compensations of hip circumduction, toe scuffing, weak prosthetic side push-off, hyperextension on the prosthetic side, higher intact side collision work, and knee osteoarthritis on the intact side. A passive prosthetic ankle-foot device replaces some of the functionalities of the biological structures of the ankle-foot system. Semi-active prostheses attempt to recover more of the biological ankle mechanics. This dissertation will focus on designing and testing two semi-active prosthetic properties of stiffness and ankle angle control: Variable Stiffness Foot (VSF) and Two-Axis aDaptable Ankle (TADA). These semi-active prostheses will be built to sense ankle angle, foot motion, and ankle moments using intrinsic position sensors, an IMU, and a load cell. Though these prosthetic sensors are limited to detecting ankle kinematics and kinetics, data will also be collected for the knee, hip,

and summative mechanics to observe the effects of the ankle-foot prosthetics on the prosthetic user. The main objective of this dissertation is to create semi-active ankle-foot prostheses based on stiffness and ankle angle control properties. It will also characterize their effectiveness using knee, hip, and summative center of mass and whole-body angular momentum.

Chapter 2. PAST WORK

(a) Introduction

The objective of the past work was to identify the significant sagittal joint mechanics that are affected by changes in forefoot stiffness using the Variable Stiffness Foot (VSF) in flat overground walking with human participants with transtibial amputation. The VSF[21] is a prosthetic foot that allows real-time modulation of forefoot stiffness during the swing phase of walking. This objective focused on exploring moments, and powers, vertical ground reaction forces, and energy and power flow through the prosthesis)[69]. Forefoot stiffness is one of the main variables that allows prosthetic users the ability to adapt their gait. Adaptable stiffness of a prosthetic ankle-foot is important as many commercially available passive prostheses are constant-stiffness devices, so a user with an adaptable stiffness prosthesis replaces the functionality of multiple commercial prostheses that each have one stiffness option.

(b) Variable Stiffness Foot (VSF) Description

The Variable Stiffness Foot (VSF)[21] offers a semi-active foot prosthesis that modulates forefoot stiffness during the swing phase. The VSF has a rigid ankle, and its forefoot acts as an overhung beam that can modulate the forefoot stiffness by adjusting a support fulcrum to change the overhang length. The VSF is a semi-active device where power is not supplied to move the body while the foot is on the ground. Instead, it supplies minimal power when the foot is in the air moving the fulcrum while the motor load is low. The fulcrum position is changed with a motor, belt, and pulley system and is positionally tracked using a potentiometer. This semi-active nature allows the VSF to be lightweight and low power compared to active prostheses, where power is supplied during foot/ground interaction. The VSF's motor commands and data collection are managed using a microcontroller [ref] with embedded software programming in the C language. The microcontroller also has an embedded inertial measurement unit (IMU) to track the foot's trajectory in real-time.

(c) Sensitivity of Joint Mechanics to Various Forefoot Stiffnesses of the Variable Stiffness Foot (VSF) in level-ground walking

This Manuscript will soon be submitted for journal consideration.

(i) Introduction

The primary function of lower limb prostheses for persons with amputation (PWA) is to restore walking on level ground. Still, they are also necessary for standing, walking on stairs and ramps, and uneven terrain. These prosthetic devices attempt to return walking functionality by mimicking some aspects of the lost human ankle-foot mechanics. This attempt to return to walking for prosthetic users is difficult as the necessary mechanics to walking are not fully understood. The difficulty in recreating the human ankle instigates a need for improved mechanical adaptability in the characteristics of the prostheses.

Energy Storage and Return (ESR) prostheses are the standard solutions to offer some passive adaptability and returned functionality to prosthetic users. ESR prostheses absorb mechanical energy using viscoelastic deformation in early/mid-stance and return it in mid/late stance. To assess the usefulness of the ESR prostheses, one proposal[12] created standardized tests to establish essential features to evaluate prosthetic feet for prescription. Another report[13] put forward that transtibial prostheses can be differentiated by two main factors: normal stiffness (superior-inferior direction to foot) and foot geometry. Interestingly, Raschke et al.[19] found that PWA preferred less stiff (normal stiffness) feet while walking, associated with 15% lower peak sagittal prosthetic socket moments. Furthermore, Fey[20] offered that decreased foot stiffness leads to an increased prosthetic range of motion (ankle), mid stance energy storage, and late stance energy return.

To further explore the effect of foot stiffness on walking mechanics, Adamczyk et al.[9] examined the hind/forefoot stiffness effects on amputee walking for various stiffnesses and walking speeds. In general, they found that a stiffer hindfoot yields decreased prosthesis energy return, larger ground reaction force (GRF) loading rate, larger knee flexion angle (stance phase), and knee extensor moment. Furthermore, they found that a stiffer forefoot yielded decreased prosthetic ankle and COM push-off

work, and larger knee extension angle and knee flexor moment in late stance. Also, Klodd et al.[10] reported that dorsiflexion angle and ankle plantarflexor moments increased with a stiffer forefoot.

To alter ankle and knee mechanics, the Variable Stiffness Foot (VSF) offers a semi-active foot prosthesis that can modulate its forefoot stiffness during the swing phase. The VSF[21] has a rigid ankle, and its forefoot acts as an overhung beam that can modulate the forefoot stiffness by adjusting a support fulcrum to change the overhang length (parameter 'a' in Figure 10). In addition, the VSF is a semi-active device – power is not supplied to move the body while the foot is on the ground, but minimal power is supplied when the foot is in the air to move the fulcrum while the motor load is low. This semi-active nature allows the VSF to be lightweight and low power compared to active prostheses, where power is supplied during foot/ground interaction. Glanzer and Adamczyk[21] reported that VSF users displayed greater energy storage and return with lower stiffnesses.

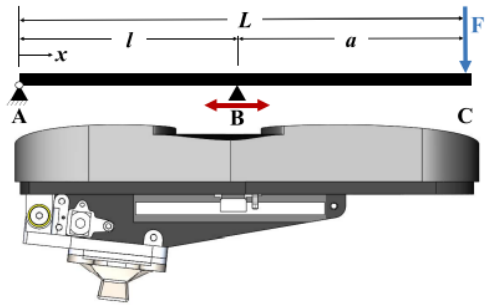

Figure 10: side drawing of the VSF highlighting the cantilever mechanics from Glanzer and Adamczyk[15] The ground reaction force on the foot acts at." F," the beam is supported at "B," and pinned at "A."

The VSF offers the ability to change forefoot stiffness during movement, and the mechanical effects of the stiffness change and its benefits to different tasks need to be experimentally determined. The VSF can be used for various walking conditions like multiple speeds, stairs, ramps, and uneven surfaces. This study focuses on characterizing the kinetic and kinematic response of participants with transtibial amputation in level overground walking, using the VSF at three different stiffnesses. Based on the findings from fixed component stiffness changes[9], we hypothesize that increasing forefoot stiffness will lead to (1) kinematic changes including decreasing peak ankle dorsiflexion and increasing peak stance-phase knee extension angles; (2) joint moment changes including increasing peak plantarflexor moment and decreasing peak knee flexor moment; (3) changes in energy and power, including decreasing trends in the magnitude of prosthetic energy storage, energy return, and peak power output; and (4) GRF

changes including increasing off-loading rate and increasing second peak of vertical ground reaction force.

(ii) Method

Seven participants (one female, seven male, ages 51.7 ± 11.9 years) with transtibial amputation were included in this study after giving written informed consent according to procedures approved by the University of Wisconsin-Madison Health Sciences Institutional Review Board (protocol #2017-0678). Participants were included under the criteria: having a unilateral transtibial amputation with stable socket fit, being at least six months post-surgery, having the ability to comfortably walk a minimum of 30 minutes without aid, and being able to walk comfortably on level ground, stairs, and ramps. Exclusion criteria included the presence of neuromuscular disorders, sores or current injuries, or surgery within the past six months. The VSF was fitted onto the participants and aligned in a medium stiffness setting by a certified prosthetist. Subjects then were given a short (10 minute) acclimation period in which they walked freely about the lab space.

The participants performed nine over-ground walking trials at 1.1 ± 0.1 m/s (approximately the typical walking speed for people with amputations[64]) with three different Variable Stiffness Foot (VSF) stiffness settings. The VSF stiffnesses were chosen as Compliant, Medium, Stiff, which were scaled to their body mass and ranged from 10 to 32 N/mm. Body mass was used for scaling stiffness to ensure that the minimum stiffness (Compliant condition as low as 10 N/mm) prevented the prosthetic keel from contacting the internal safety limit. The Stiff condition was set to be 32 N/mm, and the Medium condition was set as the halfway point of the Compliant and Stiff conditions. Body kinematics were recorded using optical motion capture (twelve Optitrack Prime 13 cameras, Natural-Point, Inc., Corvallis, OR, USA). Marker clusters were placed on each segment of both lower limbs (thighs, shanks, and feet), with additional markers placed on anatomical landmarks (medial and lateral malleoli on the intact ankle, medial and lateral epicondyles bilaterally, bony prominences of the pelvis) and specific locations on the

VSF prosthesis. Ground reaction forces were collected using two force plates (Bertec, Inc., Columbus, OH, USA). Motion capture and force plate data were recorded at 120 and 1200 Hz, respectively.

The walking speed was tracked as subjects walked across the force plates using the pelvis segment from motion capture. Trials were rejected if walking speed was more than 1.2 m/s or less than 1.0 m/s or if the feet were not cleanly on force plates, and trials continued until three successful trials were recorded in each condition. Testing was repeated similarly for the other conditions in randomized order with 5 minutes between to rest and then to acclimate to each stiffness setting by walking in the laboratory area. Stiffness settings were concealed from the participant and prosthetist by referring to them only by randomized condition numbers, although subjects could likely perceive the stiffness changes during use.

Data from one subject's compliant setting were excluded from the results due to a fault in the VSF. Also, due to an unexpected time sync problem in the instrumentation, a software fix was implemented to resample and synchronize the data for three subjects. Based on observed events from the other subjects, the first vertical ground reaction force frame before toe-off with a magnitude below 10N was synced with the maximum inferior displacement of the toe marker relative to the rest of the foot segment in the foot reference frame.

Standard lower body joint kinematics and inverse dynamics were computed using a lower-body model in Visual 3D (C-Motion, Inc., Germantown, MD, USA). Functional joint centers for the hips and knees were calculated using the Gillette algorithm to establish the rotation axis. The point along that axis representing the knee joint was determined as a projection from the midpoint of the medial and lateral epicondyles. An estimated anatomical joint center was used for the intact ankle (midpoint between malleoli). A chosen geometric location was used to specify the VSF ankle joint on the prosthetic side (0.1 m above the floor and 0.05 m anterior to the heel marker). The choice of the geometric definition of the VSF ankle was arbitrary because it lacks a true joint rotation axis; it was chosen as a systematic way to define the prosthetic ankle joint for all subjects. Leg length was measured from the floor to the greater

trochanter. The segments' masses were estimated from body mass according to standard anthropometric tables within Visual3D; prosthetic leg mass was not changed from this anthropomorphic assumption. All body segments were modeled as 6-degree-of-freedom rigid bodies.

Motion data and force data were low-pass filtered using a 4th order, bidirectional Butterworth filter with a 10 and 25 Hz cutoff, respectively. Lower-limb segment positions, segment angles, and joint angles were computed from motion capture and used to estimate the angular velocities and accelerations. Joint moments were computed from the ground reaction forces measured under each foot and inertial terms estimated from segment accelerations. Joint power was computed for the ankle, knee, and hip as the dot product of the joint moment and joint angular velocity. The prosthesis's power and energy absorption and return were calculated using the unified deformable segment model (UD power). The Unified Deformable segment model is useful as it is not sensitive to the nature of ankle joint definition. It estimates the power flowing through the ankle joint in and out of the shank without assuming rigidity of the foot. Energy storage and return in the keel were calculated as the negative and positive parts of the time integral of UD power, excluding initial heel contact (the first 20% of the stride). Initial heel impact energy was not calculated as the impact is due to the heel cushion/floor interaction and not the forefoot VSF stiffness. Energy was separated into storage (negative) and return (positive; also known as push-off) regions to investigate these separate consequences of forefoot stiffness modulation.

The results from both legs were sorted, processed, and graphed using MATLAB (The Mathworks, Natick, MA USA) in the form of hip, knee, and ankle angles, moments, and powers. Peak values of ankle dorsiflexion angle, plantarflexor moment, midstance knee extension angle, knee flexor moment, UD Power, and vertical Ground Reaction Force's (vGRF) 2nd peak were recorded, as were prosthetic energy storage, prosthetic energy return, and vGRF off-loading rate (slope of vGRF vs. time between the time-point of 250 N to the 0 N time-point[9]) were computed for each stride on the prosthetic side and were averaged across the three trials for each stiffness setting. Linear mixed-effects models were used to estimate the sensitivity of these metrics to stiffness settings, their significance (p-value), and the

coefficients of determination (r^2) of their regressions. Coefficients of determination were adjusted to account only for the explanatory value of the linear term and not the individualized offsets (random subject effects). For the sake of normalized comparability of results among subjects, all outcome measures were non-dimensionalized using the subject's body mass (M), standing leg length (L, greater trochanter to floor), and gravitational acceleration (g, 9.81 m/s/s). We used Mg for forces, MgL for work and moment, $Mg\sqrt{gL}$ for power, and $Mg\sqrt{\frac{g}{L}}$ for force rate of change[9].

Age (years)	Sex	Amputated side	Number of years post amputation (years)	Body mass (kg)	Body height (m)	Leg length(m)
70	M	L	14	83.8	1.797	0.978
61	F	R	8	63.8	1.63	0.874
34	M	R	15	77.3	1.813	0.942
46	M	R	5	104	1.896	1.06
51	M	R	8	111	1.75	0.95
44	M	L	19	75	1.72	0.93
56	M	R	3	105	1.83	0.96

Table 1: subject characteristics of age, sex, amputated side, number of years post-amputation, body mass, body height, leg length for seven subjects

(iii) Results

Joint Angle: it was hypothesized that a stiffer VSF would cause decreasing peak ankle dorsiflexion and increasing peak stance-phase knee extension angle. Our results showed during late stance; the peak dorsiflexion significantly decreased with increasing stiffness ($p=<0.0001$, $r^2=0.902$). During mid-stance, the peak knee extension angle significantly increased with increasing stiffness ($p=0.016$, $r^2=0.404$).

Prosthetic side		Non-dimensionlized										Dimensionlized								
	Peak	Comp. mean	Comp. SD	Med. mean	Med. SD	Stiff Mean	Stiff SD	Slope	Intercept	Adjusted r2	p-val of MLE	Units	Comp. mean	Comp. SD	Med. mean	Med. SD	Stiff Mean	Stiff SD	Slope	Intercept
Ankle	Dorsiflexion Angle	9.41	2.35	7.8	2.04	5.46	1.9	-2.2	12.1	0.902	<0.0001	Deg	9.41	2.35	7.8	2.04	5.46	1.9	-2.2	12.1
	Plantarflexor Moment	-0.148	0.0218	-0.148	0.0229	-0.154	0.0224	-0.00582	-0.136	0.404	0.016	Nm	-115	21.7	-121	24.9	-127	29.2	-5.62	-110
Knee	Knee Ext. Angle	-5.23	4.69	-3.69	6.29	-1.77	6.77	1.99	-7.72	0.393	0.018	Deg	-5.23	4.69	-3.69	6.29	-1.77	6.77	1.99	-7.72
	Knee Flexor	0.00107	0.0172	-0.00793	0.0197	-0.0197	0.0233	-0.0114	0.0147	0.641	0.0007	Nm	0.462	15.1	-6.94	17	-18	18.7	-10.2	12.8
GRF	Vertical 2nd peak	0.959	0.0263	0.935	0.0667	0.959	0.0833	0.0124	0.918	0.123	0.2261	N	810	181	808	155	832	179	11.4	793
	Vertical Off-loading rate	-7.49	2.76	-8.02	2.73	-8.42	3.18	-0.326	-7.42	0.23	0.0875	N/s	-6100	1980	-6880	2580	-7270	3080	-336	-6250
UD	Storage Energy	-0.0133	0.00387	-0.00937	0.0043	-0.00671	0.00308	0.0029	-0.0153	0.906	<0.0001	J	13.2	2.34	14.8	6.72	12	6.15	2.35	-12.6
	Push off Energy	0.0174	0.0055	0.0177	0.0059	0.0142	0.00547	-0.00232	0.0216	0.679	0.0003	J	-10.8	4.84	-7.75	4.17	-5.59	3.21	-1.73	17.5
	Push off Power	0.0557	0.0206	0.0568	0.0259	0.0453	0.0245	-0.00913	0.0734	0.731	0.0001	W	136	36.1	152	85.8	122	80.8	-22.3	192

Table 2: assessed biomechanical metrics with their associated means for each stiffness (Compliant, Medium, Stiff), slope of the LME regression against stiffness, mean intercept across subjects, adjusted r2, and p-value

Joint Moment: it was hypothesized that a stiffer VSF would cause increasing peak plantarflexor ankle moment and decreasing peak knee flexor moment. Our results showed during late stance, the peak plantarflexor ankle moment had an increasing trend with increasing stiffness ($p=0.018$, $r^2=0.393$). Likewise, peak knee flexor moment during midstance had an increasing trend with increasing stiffness ($p=0.0007$, $r^2=0.641$).

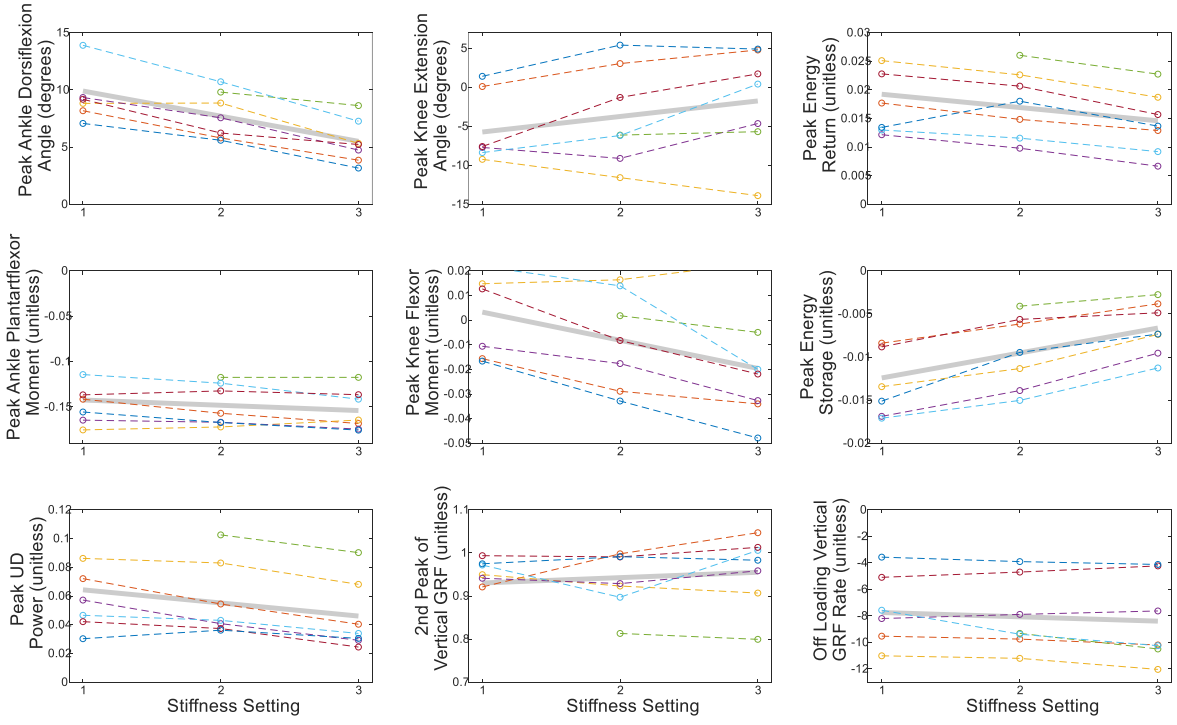

Figure 11: linear mixed-effect regressions for ankle and knee angles, moments, and UD power, energy storage and return for the non-dimensionalized data, with respect to stiffness settings. The grey bar represents the linear mixed-effects fit of all subjects. One subject didn't have data for the lowest stiffness setting.

Prosthesis energy storage, energy return, and power flow: it was hypothesized that a stiffer VSF would cause decreasing magnitudes of energy storage, energy return, and peak UD power. Our results showed a significantly decreasing magnitudes of energy storage ($p=0.0003$, $r2=0.906$), energy return ($p<0.0001$, $r^2=0.679$), and peak UD power ($p<0.0001$, $r^2=0.731$).

Ground reaction forces: it was hypothesized that a stiffer VSF would cause increasing values of the 2nd peak of vertical GRF and an increasing magnitude of GRF off-loading rate. Our results showed no significant dependence on stiffness for the 2nd peak of vGRF ($p<0.2261$, $r^2=0.123$) and the off-loading rate of the prosthetic foot ($p=0.0875$, $r^2=0.23$).

(iv) Discussion

The purpose of this study was to characterize the sensitivity of ankle and knee mechanics to various stiffnesses using an adaptable-stiffness energy storage and return (ESR) prosthetic foot (the VSF) in level-ground walking. Previous studies have presented the joint mechanics' sensitivity for various fixed sets of fore and hind-foot stiffnesses[9], identified the range of prosthetic foot stiffnesses for commercial feet[72], and introduced the design and validation of the VSF[21]. Therefore, we hypothesized that increased forefoot stiffness of the VSF would lead to specific changes in joint angles and moments, prosthesis energy, storage and return, prosthesis power, and ground reaction forces.

The results indicated that most of the hypotheses were supported. Our results (see figure 11) showed that peak magnitudes of plantarflexor ankle angle decreased, and moment increased with a stiffer VSF. Additionally, the peak knee flexor moment decreased in magnitude with the increased peak knee extension angle. The results did not support that a less stiff VSF affects the 2nd peak of the vertical ground reaction force (vGRF) and the off-loading vGRF rate. These results suggest that a less stiff VSF allows for lower ankle and knee moments, and more range of motion for ankle angles. Persons with transtibial amputations tend to have issues with knee hyperextension[31,] so a less stiff VSF can help reduce knee extension.

Previous stud[9,19] proposed that active people with transtibial amputations tend to prefer soft prostheses due to the dominance of kinetics over kinematics in ESR interactions. A less stiff (softer) VSF was associated with higher magnitudes of UD energy storage and energy return. Other research[31,44] related more prosthetic energy return with lower collision work and lower joint loads (ankle and knee moments), which potentially lowers the risk of knee osteoarthritis. Also, because the less stiff forefoot is associated with higher energy return, a less stiff forefoot could help with ground clearance due to increased leg swing acceleration[30,34,73].

In the ESR prosthetic literature, two semi-active devices specialize in giving prosthetic users the customizability to change the ankle and forefoot stiffness: Variable Stiffness Prosthetic Ankle (VSPA) and Variable Stiffness Foot (VSF). VSPA[22,36] utilizes a cam-based transmission to allow selectable nonlinear ankle torque-angle curves, which aim to mimic intact gait and modulate forefoot stiffness through motorized leaf spring configurations. VSPA allows the users to set the ankle stiffnesses according to their preferences and mobility tasks. Gait testing with VSPA had similar results of increased peak plantarflexor moment and decreased peak dorsiflexion angle with increased stiffness. Together with the present study and prior studies of fixed-component stiffness changes[9], this evidence builds up the mechanistic understanding of how parametric changes in prosthesis properties affect typical walking.

Effective control of the stiffness modulation in walking and running can be connected to the Dynamic Mean Ankle Moment Arm (DMAMA)[24]. DMAMA represents the ratio of sagittal ankle moment impulse to vertical ground reaction force impulse in stance phases of gait. The tests[24] of DMAMA showed that in natural gait, GRFs move closer to the ankle (less forward) with increased walking speed. As a follow-up, Leestma et al.[25] analyzed a subset of the data from the present study and found a positive linear sensitivity of DMAMA (more forefoot dominated) to stiffness and ground incline. Stiffness control of the VSF cannot mimic or replace kinematic control in walking, but it could influence stance to counter or enhance the effects of incline or speed. This metric, DMAMA, could be used as a control loop variable to adapt semi-active ESR prostheses to various locomotion modes like walking on

level, ramps, and stairs, and standing. DMAMA could also be used to evaluate the biomimetic performance of various passive and active prostheses.

In the present study, we did not attempt to measure or optimize the preference of the user. However, as reported in Glanzer and Adamcyk[21], users provided anecdotal comments that illustrated they were able to perceive differences in the stiffness settings, such as "I'm assuming this mode is for going down ramps." Or that the softest setting felt like "putting it in overdrive." This clear perception makes sense considering the results from a study in the VSPA foot[22], which found that individuals can detect ankle/foot stiffness variations of 7.7% with a 75% accuracy. The settings in this study spanned a factor of three, well above the minimal perception threshold, which in turn suggests that VSF variations could likely be used to adapt to a wide range of conditions that persons with TTA perceive as uncomfortable or unmanageable with traditional prostheses.

Along with stiffness, individuals also can perceive ankle damping. Azocar et al.[27] reported that PWA could perceive changes of at least 12.0% at the ankle. They also highlighted that persons with TTA[22] could perceive changes of at least 11.6% and 8% for ankle stiffness and torque, respectively. The perception of ankle damping and stiffness seem similar, but mechanically they are quite different. Varying a perceived stiffness by damping removes energy through dissipation, dramatically reducing the potential for energy return[74]. In contrast, the VSF controls how it stores and releases energy through the variation of stiffness, allowing it to maintain energy return.

Sensors are an important input in prosthetic control and past research[61,63,75] supports the validity and repeatability of inertial measurement units for measuring gait parameters. The VSF currently uses an IMU to detect when the leg is in swing phase so the stiffness could change under low loads. Upgrades to the VSF controller to improve the feedback system could include detecting kinematic variations while walking on and transitioning among speeds, level ground, ramps, stairs, and standing still. These detections could potentially be identified and investigated using machine learning algorithms[25,76].

To investigate energy storage and return in walking, Adamczyk and Kuo[31] found that push-off impairment and its related compensations are related to some asymmetries in walking for people with unilateral transtibial amputations. Lower prosthetic energy return leads to lower push-off work by the impaired limb, leading to greater energy loss in the intact leg/ground collision. Prosthesis users may compensate by adding some positive hip work during the intact and prosthetic leg stance phase. The VSF could therefore allow utilization of lower stiffnesses to allow higher energy return to minimize this compensation. Such an effect was observed with a semi-active energy-recycling prosthesis, the controlled energy storage and return (CESR) prosthesis[32]. Segal et al. [26] showed that using CESR with low stiffness increased prosthetic push-off (energy return) and decreased intact limb COM collision work compared to using a conventional foot.

It is important to investigate whether the more capable weight support of a stiffer foot or larger energy return of a compliant foot are of contrasting benefit when deciding optimal stiffness in walking. While the energy return is usually considered good and users prefer more compliant prostheses[19], there can also be a "drop-off" effect if the foot is too compliant[10]. This effect can appear as a low "effective foot length ratio" (EFLR) that fails to mimic an intact limb appropriately. For example, prostheses with short or very soft internal keels have a low EFLR, while those with longer or stiffer keels achieve EFLR closer to the physiological value[77]. This trade-off is fundamental to the mechanics of a passive compliant prosthesis, so the right choice or balance may come down to individuals' preferences or the use of semi-active, adaptable prostheses like the VSF to adjust the behavior for different circumstances. Simultaneously achieving both the low impedance and high energy return of a compliant prosthesis and the firm weight support of a stiffer foot may fundamentally require a powered foot-ankle system or a more complex mechanism such as energy recycling[23,32,33].

Beyond the prosthetic energy flow, whole body metrics like energy expenditure and center of mass mechanics (COM) must also be understood. Zelik and Adamczyk[34] showed a unified effect of ankle energy return that contributes to both leg swing and COM acceleration. Ankle energy return is a defining

characteristic of the VSF since stiffness directly affects push-off power and work. Zelik et al.[35] found that lower stiffnesses led to higher energy storage, energy return, and prosthetic limb center of mass (COM) push-off work. Walking energy expenditure in their participants with TTA was lowest for intermediate stiffness, suggesting biomechanical disadvantages to lowest stiffness despite higher energy return. Agreeing with previous results from Adamczyk and Kuo[31], people with TTA showed higher hip work with lower energy transfer from the prosthesis to the COM, which could be attributed to higher energy dissipation at the knee. These results showed that spring compliance (inverse of stiffness) influences push-off but has co-occurring biomechanical trade-off that limits how push-off can benefit the walking economy (lower metabolic cost). Additionally, Clites et al.[36] agreed that subject-preferred stiffness had no correlation with energy expenditure, but it also found that stiffness tended to be lower for self-selected speed.

Improvements to the experimental design of this research study could include increasing the number of participants, having more trials per stiffness category, and giving participants more acclimation time with the VSF for each stiffness. The VSF does not currently allow for the modulation of ankle or heel stiffness. A future step may be to build a second keel and carriage to allow for heel stiffness modulation, improving heel strike and energy storage in the early stance. Also, combining the VSF function with a repositionable ankle (e.g., Ossur Proprio) could help with ankle dorsiflexion during the swing phase to improve toe clearance and minimize tripping.

Three stiffness categories were studied in this experiment, but the VSF is capable of a continuous stiffness variation. An ideal design and control goal for the VSF is to create a continuously adaptive passive system (semi-active) that is easily perceivable. The continuously adaptive stiffness modulation will be the controller's output, and the IMU perception of locomotion mode and environment will be a main part of the feedback system. Additionally, the VSF could be used as a standardized tool for evaluating commercial passive prostheses and helping to categorize stiffness groups. Commercial prostheses vary in size, material, mechanical properties but prosthetists could use the VSF at the clinic or

as a take-home device. The VSF could be a comparison tool for selecting which passive or active prosthesis is based on their stiffness preference with everyday walking on level ground, ramps, stairs, and uneven surfaces.

(v) Conclusion

The variable stiffness foot (VSF) enables modulation of biomechanical knee and ankle outcomes through controlled modulations of forefoot stiffness. Mainly, ankle dorsiflexion angle and plantarflexor moment; knee extension angle and flexor moment; and unified deformable energy storage, energy return, and power were affected by changes in forefoot stiffness of the VSF.

Acknowledgments: This work was supported by NIH HD074424 and institutional funds from the University of Wisconsin–Madison.

(d) Published Collaboration Manuscripts

(i) A Reduced-Order Computational Model of a Semi-Active Variable-Stiffness Foot Prosthesis[78]

Authors: Michael A. McGeehan, Peter G. Adamczyk, Kieran M. Nichols, Michael E. Hahn

Abstract: Passive energy storage and return (ESR) feet are current performance standard in lower limb prostheses. A recently developed semi-active variable-stiffness foot (VSF) prosthesis balances the simplicity of a passive ESR device with the adaptability of a powered design. The purpose of this study was to model and simulate the ESR properties of the VSF prosthesis. The ESR properties of the VSF were modeled as a lumped parameter overhung beam. The overhung length is variable, allowing the model to exhibit variable ESR stiffness. Foot-ground contact was modeled using sphere-to-plane contact models. Contact parameters were optimized to represent the geometry and dynamics of the VSF and its foam base. Static compression tests and gait were simulated. Simulation outcomes were compared to corresponding experimental data. Stiffness of the model matched that of the physical VSF (R2: 0.98, root-mean-squared error (RMSE): 1.37 N/mm). Model-predicted resultant ground reaction force (GRFR) matched well under optimized parameter conditions (R2: 0.98, RMSE: 5.3% body weight,) and unoptimized parameter conditions (R2: 0.90, mean RMSE: 13% body weight). Anterior–posterior center

of pressure matched well with R2 > 0.94 and RMSE < 9.5% foot length in all conditions. The ESR properties of the VSF were accurately simulated under benchtop testing and dynamic gait conditions. These methods may be useful for predicting GRFR arising from gait with novel prostheses. Such data are useful to optimize prosthesis design parameters on a user-specific basis.

(ii) A Computational Gait Model With a Below-Knee Amputation and a Semi-Active Variable-Stiffness Foot Prosthesis[79]

Authors: Michael A. McGeehan, Peter G. Adamczyk, Kieran M. Nichols, Michael E. Hahn

Abstract: Introduction: Simulations based on computational musculoskeletal models are powerful tools for evaluating the effects of potential biomechanical interventions, such as implementing a novel prosthesis. However, the utility of simulations to evaluate the effects of varied prosthesis design parameters on gait mechanics has not been fully realized due to the lack of a readily-available limb loss-specific gait model and methods for efficiently modeling the energy storage and return dynamics of passive foot prostheses. The purpose of this study was to develop and validate a forward simulation-capable gait model with lower-limb loss and a semi-active variable-stiffness foot (VSF) prosthesis. Methods: A seven-segment 28-DoF gait model was developed and forward kinematics simulations, in which experimentally observed joint kinematics were applied and the resulting contact forces under the prosthesis evolved accordingly, were computed for four subjects with unilateral below-knee amputation walking with a VSF. Results: Model-predicted resultant ground reaction force (GRFR) matched well under trial-specific optimized parameter conditions (mean R2: 0.97, RMSE: 7.7% body weight (BW)) and unoptimized (subject-specific, but not trial-specific) parameter conditions (mean R2: 0.93, RMSE: 12% BW). Simulated anterior-posterior center of pressure demonstrated a mean R2 = 0.64 and RMSE = 14% foot length. Simulated kinematics remained consistent with input data (0.23 deg RMSE, R2 > 0.99) for all conditions. Conclusions: These methods may be useful for simulating gait among individuals with lower-limb loss and predicting GRFR arising from gait with novel VSF prostheses. Such data are useful to optimize prosthesis design parameters on a user-specific basis.

(e) Development of VSF with hind and forefoot properties

The VSF allows for adaptable fore-foot stiffness modulation and has been shown to affect the knee and ankle mechanics. The VSF's ankle is rigid, and the forefoot mainly affects mid to late prosthetic stance. Adamczyk et al.[14] examined both hind and forefoot stiffness effects on persons with transtibial amputations walking for various controlled stiffnesses and walking speeds. They found similar ankle and knee mechanical effects as was seen in the VSF results, but they also showed that a stiffer hindfoot yields decreased prosthesis energy return, larger ground reaction force (GRF) loading rate, larger knee flexion angle (stance phase), and knee extensor moment.

To improve prosthetic walking adaptability, some of my work involved working with a team of students to upgrade the VSF design to include two keels (VSF2K): one forefoot and one hindfoot. The overhung beam (keel) and carriage system for the original VSF were replicated and shrunk for the hindfoot. The two keels are mounted at a common axis near the ankle (see figure 12) and are diagonally extended downwards to mimic the midfoot arch. Two motors will move the hind and forefoot carriages to change the hind and forefoot stiffness of the VSF2K. The foot stiffness was designed to range from 7 to 30 N/mm.

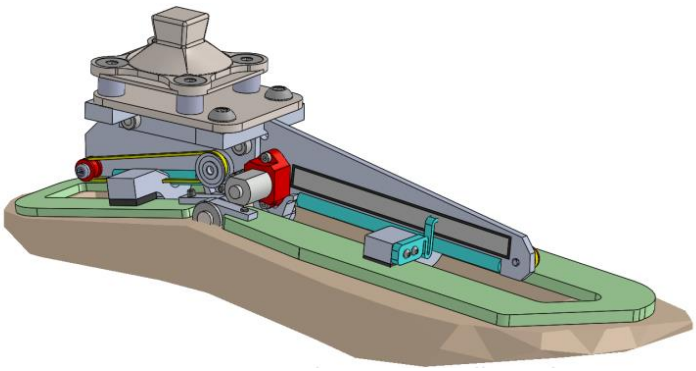

Figure 12: proposed design of the Variable Stiffness Foot with two keels (VSF2K)

The collection and construction of the individual parts are nearly complete, and other students are currently assembling them for the first physical build of the VSF2K. Future steps for those students will include developing the VSF2K software controller to modulate the hind and fore-foot stiffness and testing its effects on humans. Feedback for control will involve foot IMU motion reconstruction, motor control to move the carriage, and potentiometer readings of carriage position to change the stiffness. Tests will include many of the same outcomes observed in the study described here, as well as effects due to hindfoot stiffness and tests on non-level terrain.

(f) Conclusion

This past work explored the effect of three stiffnesses (compliant, medium, and stiff) of the Variable Stiffness Foot on the sagittal ankle and knee angles, moments, and powers, vertical ground reaction forces, and unified deformable energy and power. Forefoot stiffness is one of the main variables that allows prosthetic users to adapt their functional gait, and another main variable is ankle angle control. A computational contact model was developed for the VSF to replicate its energy return and storage properties, and it predicted the resultant and center of pressure of the ground reaction force under the prosthesis. Additionally, a Variable Stiffness Foot with two keels (VSF2K) was designed to allow for hind and fore-foot stiffness modulation. The specific aims and methods will be proposed in the following section, “Current and Future Work.” The ankle angle control will be investigated using the Two-Axis aDaptable Ankle (TADA) prosthesis.

Chapter 3. CURRENT AND FUTURE WORK

(a) Objective of Current and future work

This current and future work of the dissertation will advance development on a two-degree freedom ankle prosthesis with adjustment of plantarflexion/dorsiflexion and inversion/eversion. The main hypothesis is that controlled modulation of ankle angle will affect joint and whole-body mechanics as specified below while walking with the new generation of Two-Axis aDaptable ankle (TADA). Participants with no amputations (non-disabled) and persons with unilateral transtibial amputations will walk on flat and inclined surfaces with the TADA at fixed neutral and adaptable ankle angles.

(b) TADA description

The Two-Axis aDaptable Ankle (TADA)[8] is a semi-active ankle prosthesis that can independently modulate two axes of ankle angles (sagittal and frontal). It can support reaction forces in all directions and prevent rotations of the attached foot when the motor shaft is not moving. The TADA has a U-joint that houses a system of two wedge cams rotated by two motors pointing toward each other (design principles similar to the previous design shown in figure 13). The wedge cam mechanism has two short cylinders (wedge cams) pressed on each other, aligned with the U-joint's longitudinal axis, and free

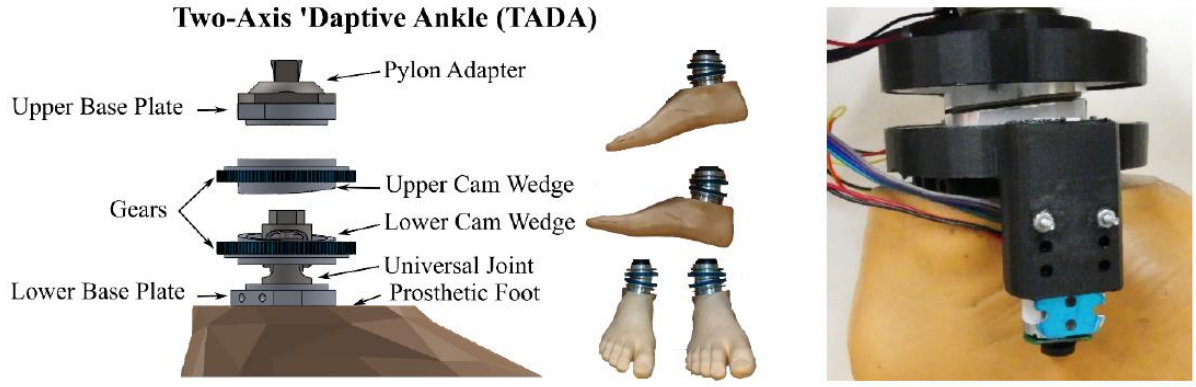

Figure 13: Previous design of the Two-Axis Adaptable Ankle (TADA) taken from Adamczyk[8]

to rotate about the cylindrical axis. The two cylinders have mating faces inclined at five degrees that can tolerate large compressive forces like multiples of body weight and create enough friction to counter the back-driving moment allowing non-backdrivability. These relative orientations of the inclined mating

faces allow the TADA to produce a variety of sagittal and frontal ankle angles (see figure 14). The previous version and the TADA can be mounted on the residual limb by a pyramid adaptor and can use any prosthetic foot.

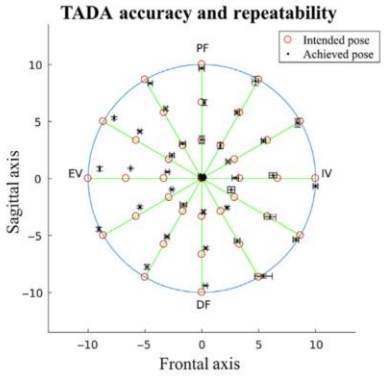

Figure 14: ankle angle accuracy of the previous build of Two-Axis aDaptable Ankle (TADA) from Adamczyk[8]. Mean position error (sagittal and frontal) magnitude was less than 0.4 deg.

The TADA[80] will have two integrated inertial measurement sensors mounted one on each half of the U-joint to reconstruct real-time foot and shank movement. In addition, a load cell sensor (Europa+ Smart Pyramid) will measure axial ankle force and two-axis ankle moments (sagittal and frontal) with the streaming of load data by Bluetooth LE. Data will be sent to a Raspberry Pi Model 4B, operating a Linux operating system. The software architecture will be controlled by the Robotic Operating System (ROS) program modules (nodes). Nodes will be dedicated to various controlling parts and involve dual motor control with encoder and hall sensor feedback, IMU motion reconstruction, data collection, user interface, and gait detection. The software scripts will be written in Python and C++.

The TADA electronics will be powered by one 12 V lithium polymer Battery (120C, 1.5Ah). Wires will supply current to a circuit board with one wire supplying 12V to the 2 Faulhaber brushless DC motors. Another wire will connect to a step-up voltage regulator (12 to 24V), providing two safe torque off lines and a power line to the motor driver. The motor driver will power the encoders and hall sensors of the motors with 5V wires. Another wire from the circuit board will connect to a step-down voltage regulator (12 to 5V) that will power the raspberry pi computer. Most of the electronics will be mounted to a waist pack that will house the motor drivers, raspberry pi, battery, voltage regulators, and circuit board. The wires will be bundled and strapped to the leg around the thigh and below the knee to power the motor system (motors, encoders, hall sensors) located in the TADA prosthetic.

An inertial measurement unit (IMU) will be consistently placed on the anterior portion near the toes of a low-profile prosthetic foot. The prosthetic foot will be rigidly attached to the TADA. The

feedback system of the TADA will involve the load cell for ankle forces and moments, IMU for motion reconstruction, and motor encoders and hall sensors for ankle angle.

(c) Specific Aims

1. *Develop and test the kinematic and kinetic validation of the Two-Axis aDaptable Ankle (TADA) feedback controller system.*

The objective of specific aim 1 is to complement the mechanical hardware upgrades of the TADA with software controllers that ensure the control laws are followed. The control laws were determined from common walking issues of persons with transtibial amputation. These issues include lifting the toe during every swing phase, anticipatory slope-matching control, and moment-limiting control. This aim will validate the TADA controller's ability to detect kinematic and kinetic variables and effectively change ankle angle control. In addition, the aim will focus on prosthetic walking in non-disabled persons using lateral prosthetic extension boots with the TADA. This aim will compare the adaptable TADA and the neutral TADA (fixed angle) and be broken into two parts: a) Kinematic validation of ankle angle with sufficient sagittal toe lift and low difference between ankle angle and floor angle (foot angle matches the floor angle); and b) Kinetic validation of orientation with minimization of the mean absolute resultant of sagittal and frontal ankle moments relative to a specific target ankle moment (non-zero).

The kinematic aim hypothesizes that there will be no difference between the control of the prosthetic ankle angle and the intact ankle angle trajectory during the swing phase, and that there will be no difference between the mean prosthetic ankle angle and the pre-recorded ground slope during the stance phase. The kinetic aim hypothesizes that the means of the sagittal and frontal prosthetic ankle moments will be less than a fixed neutral ankle's means.

2. *Evaluate the biomechanical effects of the TADA on out-of-the-lab walking while having the main control laws of lifting the toe during every swing phase, anticipatory slope-matching control, and moment-limiting control*

The main objective of specific aim 2 is to evaluate the mechanical responses (sagittal and frontal) using the TADA design and controllers from aim 1 on out-of-the-lab walking. Persons with unilateral transtibial amputations will walk on the TADA for a set of several experiments.

a) Toe lift during every swing phase

We will test participants walking on level and sloped ground at various speeds. This sub-aim will be to sagittally control ankle angle during the swing phase to increase minimum toe clearance. We hypothesize that minimum toe clearance will increase at first due to the initial adaptation to the TADA's controller, then decrease over time as the participants relax the height of their steps, and that therefore, the residual knee angle will be straighter during swing using the adaptable ankle as opposed to the neutral ankle. If successful, this controller will be a component of the other controllers.

b) Anticipatory slope matching control

We will test participants walking on square laps (uphill, downhill, cross, diagonal walking) on a sloped surface. This sub-aim will be to change the ankle angle to decrease the mean difference between foot orientation and ground angle. We hypothesize that the absolute mean resultant ankle moment will be less using the adaptable ankle than the neutral ankle.

c) Moment limiting control

We will test participants walking on square laps on a sloped surface. This sub-aim will be to change the ankle angle to decrease the mean absolute ankle moment to a lower specific target (non-zero magnitude). We hypothesize that the difference between foot and ground angles will be less using the adaptable ankle than the neutral ankle.

(d) Methods

1. *Aim 1 method: TADA kinematic and kinetic testing with non-disabled persons walking with a prosthesis testing orthosis*

Four participants with no amputations who are non-disabled walkers will be included in this study after giving written informed consent according to procedures approved by the University of Wisconsin-Madison Health Sciences Institutional Review Board (protocol #2020-0812). Participants will be included under the criteria: comfortably walk a minimum of 30 minutes without aid and walk on level ground and ramps. Exclusion criteria include the presence of neuromuscular disorders, sores or current injuries, amputations, or surgery within the past six months.

The TADA will be fitted onto the participants using a custom-made attachment boot, where the TADA will be mounted laterally to the participant's right foot. The TADA will be aligned in a neutral configuration (comfortable static sagittal angle of foot to lower leg and no inversion/eversion). Subjects then will be given a short (10 minute) acclimation period in which they walk freely about the lab space. Aim 1 will be broken up into two sets of methods: 1a) Kinematic validation of ankle angle with sufficient sagittal toe lift and low difference between ground slope and foot angle and 1b) Kinetic validation of ankle angle with minimization of sagittal and frontal ankle moments relative to a lower specific target (non-zero magnitude).

Aims 1a and 1b will have similar methods as described below.

i. Walk across two force plates in motion capture lab at three different speeds (0.8, 1.2, 1.6m/s)
ii. Walk on an inclined treadmill (-5, 0, and 5 deg) at a consistent self-selected speed
iii. Walk on a 5-degree ramp (uphill, downhill, diagonal) at a self-selected speed

Aim 1a will test the feedback system checking the computed kinematic variables against known values (speed and slope values). Aim 1b will test the feedback system checking the computed kinematic (speed and slope values) and kinetic (ankle moment) variables. Both aim 1a and 1b will alter their respective mechanical variables by changing ankle angle. The participant will use the TADA at a neutral angle and then with an adaptable angle. The TADA will have integrated load cell feedback for Aim 1b.

The instrumentation will detect the primary variables of concern: minimum toe clearance, difference between ground slope and foot angle, walking speed, DMAMA, and mean absolute resultant sagittal and frontal ankle moments. Secondary variables will be computed using the motion capture cameras, force plate, and inertial measurement unit (IMU) bodysuit (Xsens suit[81]). The Xsens suit includes 17 inertial measurement units synced together and radio-transmits data to the computer. The secondary variables will include joint sagittal angles, margin of stability, step width, frontal angular momentum, knee angle and moments, and hip angle, moments, and work.

2. Aim 2 method: TADA testing with persons with transtibial amputations

Ten Participants with trans-tibial amputations will be included in this study after giving written informed consent according to procedures approved by the University of Wisconsin-Madison Health Sciences Institutional Review Board (protocol #2020-0812). Participants will be included under the criteria: having a unilateral transtibial amputation with stable socket fit, being at least six months post-surgery, having the ability to comfortably walk a minimum of 30 minutes without aid, and having the ability to walk on level ground comfortably, stairs, and ramps. Exclusion criteria included the presence of neuromuscular disorders, sores or current injuries, or surgery within the past six months. The TADA will be fitted onto the participants by a certified prosthetist and aligned to a neutral configuration (comfortable static sagittal angle of foot to lower leg and no inversion/eversion). Subjects then will be given a short (10 minute) acclimation period in which they will walk freely about the lab space. An outside-of-the-lab route at self-selected walking speed will involve:

i. Walking on flat and sloped ground (0, -5, 5 deg) with the toe lift controller
ii. Walking two sets of square laps on a sloped surface (see figure 15) with the anticipatory slope-matching controller

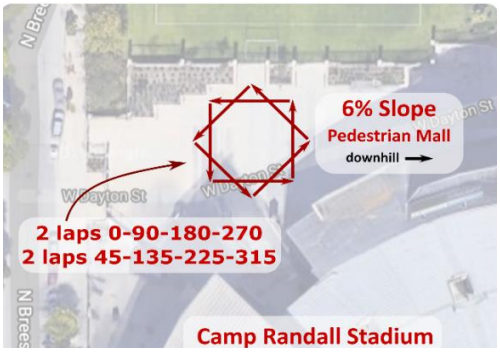

Figure 15: map describing the sets of two square laps on an outside-of-the-lab hill taken from TADA's grant document[73]

iii. Walking two sets of square laps on a sloped surface (one square is rotated 45 deg) with the moment-limiting controller

One set of square laps will be uphill, cross hill, downhill, and cross hill. The other set will rotate the previous set 45 degrees to demand mixed angles (e.g., combinations of dorsiflexion and inversion) relative to the walking direction (see figure 15). The participant will use the TADA in a neutral ankle and then with an adaptable ankle. Instrumentation will detect the primary variables of concern: the minimum toe clearance, walking speed, difference between ground slope and foot angle, DMAMA, and mean absolute resultant sagittal and frontal ankle moments. Secondary variables will be collected using the Xsens IMU suit. They will include joint sagittal angles, margin of stability, step width, and frontal angular momentum.

3. Kinematic and kinetic data collection and processing

For Aim 1a, body kinematics using the lab equipment will be recorded using optical motion capture (twelve Optitrack Prime 13 cameras, Natural-Point, Inc., Corvallis, OR, USA). Marker clusters will be placed on each segment of both lower limbs (thighs, shanks, and feet), with additional markers placed on anatomical landmarks (medial and lateral malleoli on the intact ankle, medial and lateral epicondyles bilaterally, bony prominences of the pelvis) and specific locations on the TADA prosthesis. Ground reaction forces will be collected using two force plates (Bertec, Inc., Columbus, OH, USA). For Aim 1, Motion capture and force plate data will be both recorded at 200Hz. The walking speed will be tracked as subjects walk across the force plates using the pelvis segment from motion capture. Trials will be rejected if walking speed is more than 0.1 m/s above or below the target walking speed or if the feet were not cleanly on force plates. The trials will continue until three successful trials are recorded in each condition. Then, testing will be repeated similarly for the other conditions in randomized order with a few minutes rest between each change of speed/incline/condition.

Standard lower body joint kinematics and inverse dynamics will be computed using a lower-body model in Visual 3D (C-Motion, Inc., Germantown, MD, USA). The Gillette algorithm will calculate functional joint centers for the hips and knees to establish the rotation axis. The point along that axis

representing the knee joint will be determined as a projection from the midpoint of the medial and lateral epicondyles. The prosthetic ankle joint will be defined as the center point between the two cam wedges for the TADA. Leg length will be measured from the floor to the greater trochanter. Masses of the segments will be estimated from body mass according to standard anthropometric tables within Visual3D; prosthetic leg mass will not be changed from this anthropomorphic assumption. All body segments will be modeled as 6-degree-of-freedom rigid bodies.

Motion data and force data will be low pass filtered using a 4th order, bidirectional Butterworth filter with a 10 and 25 Hz cutoff, respectively. Lower-limb segment positions, segment angles, and joint angles will be computed from motion capture and will be used to estimate angular velocities and accelerations. The joint moments will be calculated from the force plate and load cell depending on the aim and inertial terms estimated from segment accelerations. The Joint power will be computed for the ankle, knee, and hip as the dot product of the joint moment and joint angular velocity. The prosthesis's power, energy absorption, and return will be calculated using the unified deformable segment model (UD power). The Unified Deformable segment model[69] is useful as it is not sensitive to the nature of ankle joint definition. It estimates the power flowing through the ankle joint in and out of the shank without assuming rigidity of the foot.

The results from both legs will be sorted, processed, and graphed using MATLAB (The Mathworks, Natick, MA USA). They will consist of the peaks of the sagittal and frontal ankle dorsiflexion/inversion angle and plantarflexor/invertor moments, peak knee extension angle, mean DMAMA, minimum toe clearance, walking speed, mean difference between ground slope and foot angle, mean margin of stability, mean step width, and mean frontal angular momentum. Linear mixed effects models will be used to estimate the sensitivity of these metrics to stiffness, angle, and speed, their significance (p-value), and the coefficients of determination (r^2) of their regressions. For the sake of normalized comparability of results among subjects, all outcome measures will be non-dimensionalized using the subject's body mass (M), standing leg length (L, greater trochanter to floor), and gravitational

acceleration (g, 9.81 m/s/s). We used Mg for forces, MgL for work and moment, $Mg\sqrt{gL}$ for power, and $Mg\sqrt{\frac{g}{L}}$ for force rate of change [9].

(e) Conclusion

This section explored the specific aims and methods necessary to design, build, and investigate the biomechanical effects of modulating the ankle angle of the Two-Axis aDaptable Ankle (TADA). This work will be performed over the next two years as outlined in the following "Timeline" section.

(f) Impact of Proposed Work

The proposed work will develop the TADA device and controller and test the biomechanical effects of TADA prosthetic walking over flat and sloped surfaces. The TADA's multi-axis control is important as it offers adaptable frontal and sagittal angles to potentially adjust to various locomotion modes like turning, acceleration, stairs, and rocky terrain. In addition, the real-time controller offers step-by-step adjustments which could minimize joint loads, increase push-off, and adjust to user preference. The controller could also be developed to sense the various locomotion modes and adapt to locomotion transitions like walk-to-stand and slow-to-fast walking. Another benefit is the TADA's ability to combine with other low-profile passive and semi-active prostheses. For example, a split toe prosthesis could be attached to improve turning and rocky terrain walking. The TADA could also be combined with the VSF2K to mix the adaptable angle control with the adjustable hind and forefoot stiffness modulation.

The TADA could offer two types of adaptation: preemptive and responsive. The preemptive adaptation consists of a feedforward controller adjusting the ankle angle to match the known ground slope. Future development could involve detecting ground slope. The potential first steps to detecting ground slope could be to include more lower-leg IMUs[68] and to use machine learning to identify key mechanical walking features for different slopes[82,83]. The response adaptation involves a feedback moment-limiting controller that detects ankle moments using the load cell and adjusts the ankle angle to decrease mean ankle moments to a non-zero target value. Preemptive adaptation allows prosthetic users to

adjust their walking if the environment is predictable. In contrast, responsive adaptation is important for improved adjustment to unpredictable and inconsistent terrain.

The TADA can be converted to a powered prosthesis where adjustable positive power can be applied during the stance phase. This conversion may involve replacing the friction interfaces with bearings and utilizing more powerful motors with higher torque outputs.

This dissertation will contribute the work for the TADA's two-axis prosthesis control to a collaborative grant called "Multi-axis prosthesis control through an osseointegrated neural interface[80]." Future TADA work will further optimize the mechanical ankle (smaller and lighter) and be designed to fit onto a sheep's residual leg. It will be called the Sheep Two-Axis aDaptable Ankle (STADA). The STADA work aims to incorporate an osseointegrated bidirectional neural interface into the prosthetic instrumentation. The osseointegration is an alternative to prosthetic socket attachment and could eliminate socket suffering due to the direct attachment of the living bone and load-bearing prosthetic implant. The bidirectional neural interface could send and receive signals between the user and prosthesis to adjust and sense the ankle angle. The main aim of the STADA work will be to demonstrate proof of principle that a semi-active and multi-axis prosthesis like the STADA could be neurally controlled.

Chapter 4. TIMELINE

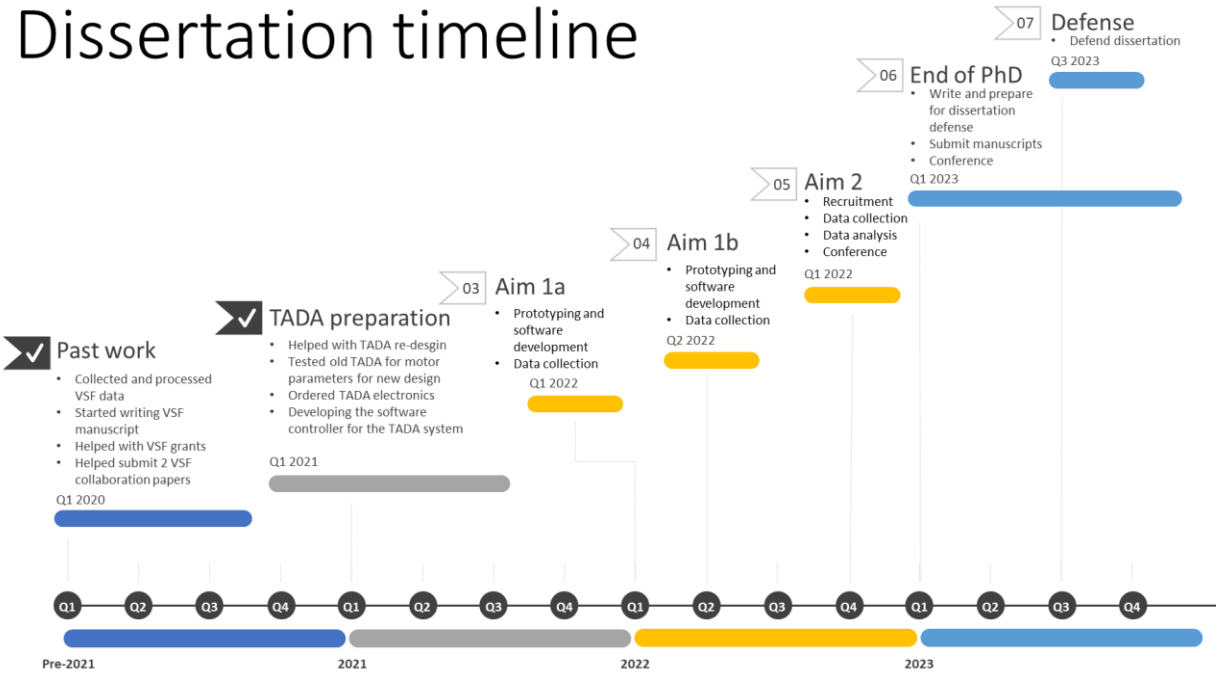

Figure 16: timeline graphic displaying the progress of dissertation work from pre-2021 to 2023

(a) Past work (Pre-2021)

Collected and processed VSF data

Started writing the VSF manuscript

Helped with VSF grants

Helped submit 2 VSF collaboration papers

(a) Current and Future Work (Jan 2021 - May 2023)

Preparation (Jan 2021 - Apr 2022)

Submit VSF manuscript (present)

Helped with TADA re-design

Tested old TADA for motor parameters for new design

Ordered TADA electronics

Developing the software controller for the TADA system (present)

Have a functional TADA with working motors, encoders, and hall sensors (1 month)

Finish develop ROS controller on the raspberry pi and Vacation (1 month)

Integrate 2 IMUs into ROS controller and start setting up motion reconstruction (1 month)

Set up mounting for electronics mounting and finish test mechanical and electronics systems of TADA (1 month)

Aim 1 (May 2022 - Dec 2022)

Prototyping and software development (2 months)

Data collection and Vacation (1 month)

Prototyping and software development (2 months)

Data collection and conference (1 month)

Data analysis (1 month)

Manuscript Writing and Vacation (1 month)

Aim 2 (Jan 2023 - May 2023)

Recruitment and protocol creation (1 month)

Data Collection (2 months)

Data analysis (1 month)

Manuscript Writing (1 month)

(b) End of Ph.D. (June 2023 - Dec 2023)

Adapt hardware and software of TADA to create TADA for Sheep (STADA) (2 months)

Preparation and writing for dissertation defense (1 month)

Vacation and Conference (1 month)

Career applications and interviews (1 month)

Defend dissertation (1 month, Nov 2023)

Update dissertation document, finalize and submit manuscripts (1 month)

Chapter 5. NOMENCLATURE

Abbreviations	Definition
AOPA	American Orthotic and Prosthetic Association
BOS	Base of Support
BW	Body Weight
CAREN	Computer Assisted Rehabilitation ENvironment
CESR	Controlled Energy Storage and Return
COM	Center of Mass
COP	Center of Pressure
DMAMA	Dynamic Mean Ankle Moment Arm
DOD	Department of Defense
EFLR	Effective Foot Length Ratio
ESR	Energy Storage and Release
GRF	Ground Reaction Force
GRFR	Ground Reaction Force Resultant
IMU	Inertial Measurement Unit
KEAM	Knee External Adductor Moment
LE	Low Energy
LME	Linear Mixed Effects
MATLAB	MATrix LABoratory
MOS	Margin of Stability
MTC	Minimum Toe Clearance
PWA	Person with Amputation
RMSE	Root Mean Squared Error
ROS	Robotic Operating System
STADA	Sheep Two Axis aDaptable Ankle
TADA	Two Axis aDaptable Ankle
TTA	Transtibial Amputation (unilateral)
UD	Unified Deformable
vGRF	vertical Ground Reaction Force
VSF	Variable Stiffness Foot
VSPA	Variable Stiffness Prosthetic Ankle
xCOM	extrapolated Center of Mass

Units	
Angle	Degrees (deg)
Moment	Newton-meter (Nm)
Power	Watts (W)
Energy/Work	Joules (J)
Vertical GRF	Newtons (N)
Vertical off-loading rate	Newton/second(N/s)

Chapter 6. LISTS OF FIGURES AND TABLES

(a) List of Figures

Figure 1: graphical representation of gait events of a non-disabled person and person with a prosthetic leg from Rajukova et al.[7] 2
Figure 2: Non-disabled ankle moment vs. angle of the stance phase of typical walking from Safaeepour et al.6 Stance phase starts with controlled plantarflexion, transitions to controlled dorsiflexion, and ends with powered plantarflexion. Stiffness relates to the slope of ankle moment and angle. 3
Figure 3: Various considerations in developing passive, active, and semi-active prostheses from Adamczyk[8] 3
Figure 4: linear mixed model trends showing the relationships of prosthetic forefoot stiffness on DMAMA for various locomotion modes from Leestma et al.[18] The persons with transtibial amputations walked on level ground, up and down ramps, and up and downstairs. Color lines represent the subject-independent linear mixed effect regressions. Gray markers, vertical bars, and lines show each person's average, standard deviation, and subject-specific linear fit. The asterisk (*) represents a significant linear trend (p-value < 0.05). 7
Figure 5: Net metabolic rate as a function of measured scuff impulse and toe lift height from Wu et al.[24] The toe clearance height and scuff impulse were normally distributed, meaning that more of the scuffs had low magnitude scuffs and low lift height 9
Figure 6: Normalized socket reaction moment in response to frontal (coronal) angular and translational socket changes from Boone et al.[36] The frontal socket reaction moments were shown for angular perturbations (Graph A) and translational perturbations (Graph B). 12
Figure 7: sagittal and frontal representations (A and B) of prosthetic and intact side collision and push-off. Graphs of vertical GRF (C), prosthetic foot-ankle power (D), and intact knee external adduction moment (E) vs. percentage of stride were shown from Morgenroth et al.[41] 13
Figure 8: conceptual diagram (A) and numerical graph (B) showing the relationship of the center of mass (COM) mediolateral position, extrapolated COM (xCOM), base of support (BOS), and margin of stability (MOS) from Beltran et al.[46] 14
Figure 9: Motion reconstruction steps with representative data trajectories from Rebula et al.[57] 17
Figure 10: side drawing of the VSF highlighting the cantilever mechanics from Glanzer and Adamczyk15 The ground reaction force on the foot acts at." F," the beam is supported at "B," and pinned at "A." 22
Figure 11: linear mixed-effect regressions for ankle and knee angles, moments, and UD power, energy storage and return for the non-dimensionalized data, with respect to stiffness settings. The grey bar represents the linear mixed-effects fit of all subjects. One subject didn't have data for the lowest stiffness setting. 27
Figure 12: proposed design of the Variable Stiffness Foot with two keels (VSF2K) 35
Figure 13: Previous design of the Two-Axis Adaptable Ankle (TADA) taken from Adamczyk[8] 37
Figure 14: ankle angle accuracy of the previous build of Two-Axis aDaptable Ankle (TADA) from Adamczyk[8]. Mean position error (sagittal and frontal) magnitude was less than 0.4 deg. 38
Figure 15: map describing the sets of two square laps on an outside-of-the-lab hill taken from TADA's grant document[73] 42
Figure 16: timeline graphic displaying the progress of dissertation work from pre-2021 to 2023 47

(b) List of Tables

Table 1: subject characteristics of age, sex, amputated side, number of years post-amputation, body mass, body height, leg length for seven subjects 26
Table 2: assessed biomechanical metrics with their associated means for each stiffness (Compliant, Medium, Stiff), slope of the LME regression against stiffness, mean intercept across subjects, adjusted r2, and p-value 27

Chapter 7. REFERENCES

1. Lower limb amputations – Epidemiology and assessment – PM&R KnowledgeNow. https://now.aapmr.org/lower-limb-amputations-epidemiology-and-assessment/.
2. Ziegler-Graham, K., MacKenzie, E. J., Ephraim, P. L., Travison, T. G. & Brookmeyer, R. Estimating the Prevalence of Limb Loss in the United States: 2005 to 2050. *Arch. Phys. Med. Rehabil.* **89**, 422–429 (2008).
3. Dillingham, T. R., Pezzin, L. E. & Shore, A. D. Reamputation, mortality, and health care costs among persons with dysvascular lower-limb amputations. *Arch. Phys. Med. Rehabil.* **86**, 480–486 (2005).
4. Wanamaker, A. B., Andridge, R. R. & Chaudhari, A. M. W. Projected Health Care Associated Costs of Workplace-Related Traumatic Amputation After 10, 15, and 20 Years: Part I: Lower Limb. *JPO J. Prosthet. Orthot.* **31**, 189–198 (2019).
5. Vu, H. T. T. *et al.* A Review of Gait Phase Detection Algorithms for Lower Limb Prostheses. *Sensors* **20**, 3972 (2020).
6. Safaeepour, Z., Esteki, A., Ghomshe, F. & Abu Osman, N. Quantitative analysis of human ankle characteristics at different gait phases and speeds for utilizing in ankle-foot prosthetic design. *Biomed. Eng. OnLine* **13**, 19 (2014).
7. Rajťúková, V., Michalíková, M., Bednarčíková, L., Balogová, A. & Živčák, J. Biomechanics of Lower Limb Prostheses. *Procedia Eng.* **96**, 382–391 (2014).
8. Adamczyk, P. G. Chapter 9 - Semi-active prostheses for low-power gait adaptation. in *Powered Prostheses* (eds. Dallali, H., Demircan, E. & Rastgaar, M.) 201–259 (Academic Press, 2020). doi:10.1016/B978-0-12-817450-0.00009-2.
9. Adamczyk, P. G., Roland, M. & Hahn, M. E. Sensitivity of biomechanical outcomes to independent variations of hindfoot and forefoot stiffness in foot prostheses. *Hum. Mov. Sci.* **54**, 154–171 (2017).
10. Klodd, E., Hansen, A. H., Fatone, S. & Edwards, M. Effects of prosthetic foot forefoot flexibility on gait of unilateral transtibial prosthesis users. *J. Rehabil. Res. Dev.* **47**, 899–910 (2010).
11. Lehmann, J. F., Price, R., Boswell-Bessette, S., Dralle, A. & Questad, K. Comprehensive analysis of dynamic elastic response feet: Seattle ankle/lite foot versus SACH foot. *Arch. Phys. Med. Rehabil.* **74**, 853–861 (1993).
12. AOPA. *Prosthetic Foot Project Report*. https://www.aopanet.org/wp-content/uploads/2013/12/Prosthetic_Foot_Project.pdf (2010).
13. Major, M. J., Twiste, M., Kenney, L. P. J. & Howard, D. Amputee Independent Prosthesis Properties—A new model for description and measurement. *J. Biomech.* **44**, 2572–2575 (2011).
14. Foort, J. Alignment of the above-knee prosthesis. *Prosthet. Orthot. Int.* **3**, 137–139 (1979).
15. Endolite Elan. *Endolite Elan* http://www.endolite.com/products/elan.
16. Kinnex. *Freedom Innovations* http://www.freedom-innovations.com/kinnex/.
17. Meridium. https://www.ottobockus.com/prosthetics/lower-limb-prosthetics/solution-overview/meridium/.
18. Ossur Products: Feet. *Össur* https://www.ossur.com/prosthetic-solutions/products/all-products/feet (2019).
19. Raschke, S. U. *et al.* Biomechanical characteristics, patient preference and activity level with different prosthetic feet: A randomized double blind trial with laboratory and community testing. *J. Biomech.* **48**, 146–152 (2015).
20. Fey, N. P. The influence of prosthetic foot design and walking speed on below-knee amputee gait mechanics. (2011).
21. Glanzer, E. M. & Adamczyk, P. G. Design and Validation of a Semi-Active Variable Stiffness Foot Prosthesis. *IEEE Trans. Neural Syst. Rehabil. Eng.* **26**, 2351–2359 (2018).
22. Shepherd, M. K. & Rouse, E. J. The VSPA Foot: A Quasi-Passive Ankle-Foot Prosthesis With Continuously Variable Stiffness. *IEEE Trans. Neural Syst. Rehabil. Eng.* **25**, 2375–2386 (2017).
23. Quraishi, H. A. *et al.* A passive mechanism for decoupling energy storage and return in ankle–foot prostheses: A case study in recycling collision energy. *Wearable Technol.* **2**, (2021).

24. Adamczyk, P. G. Ankle Control in Walking and Running: Speed- and Gait-Related Changes in Dynamic Mean Ankle Moment Arm. *J. Biomech. Eng.* **142**, 071007 (2020).
25. Leestma, J. K., Fehr, K. H. & Adamczyk, P. G. Adapting Semi-Active Prostheses to Real-World Movements: Sensing and Controlling the Dynamic Mean Ankle Moment Arm with a Variable-Stiffness Foot on Ramps and Stairs. *Sensors* **21**, 6009 (2021).
26. Shepherd, M. K., Azocar, A. F., Major, M. J. & Rouse, E. J. Amputee perception of prosthetic ankle stiffness during locomotion. *J. NeuroEngineering Rehabil.* **15**, 99 (2018).
27. Azocar, A. F., Shorter, A. L. & Rouse, E. J. Damping Perception During Active Ankle and Knee Movement. *IEEE Trans. Neural Syst. Rehabil. Eng.* **27**, 198–206 (2019).
28. Ingraham, K. A., Choi, H., Gardinier, E. S., Remy, C. D. & Gates, D. H. Choosing appropriate prosthetic ankle work to reduce the metabolic cost of individuals with transtibial amputation. *Sci. Rep.* **8**, 15303 (2018).
29. Rose, J. & Gamble, J. G. *Human walking*. vol. 3 (Williams & Wilkins Baltimore, 1994).
30. Wu, A. R. & Kuo, A. D. Determinants of preferred ground clearance during swing phase of human walking. *J. Exp. Biol.* jeb.137356 (2016) doi:10.1242/jeb.137356.
31. Adamczyk, P. G. & Kuo, A. D. Mechanisms of Gait Asymmetry Due to Push-Off Deficiency in Unilateral Amputees. *IEEE Trans. Neural Syst. Rehabil. Eng.* **23**, 776–785 (2015).
32. Collins, S. H. & Kuo, A. D. Recycling Energy to Restore Impaired Ankle Function during Human Walking. *PloS One* **5**, e9307 (2010).
33. Segal, A. D., Orendurff, M. S., Czerniecki, J. M., Schoen, J. & Klute, G. K. Comparison of transtibial amputee and non-amputee biomechanics during a common turning task. *Gait Posture* **33**, 41–47 (2011).
34. Zelik, K. E. & Adamczyk, P. G. A unified perspective on ankle push-off in human walking. *J. Exp. Biol.* **219**, 3676–3683 (2016).
35. Zelik, K. E. *et al.* Systematic Variation of Prosthetic Foot Spring Affects Center-of-Mass Mechanics and Metabolic Cost During Walking. *IEEE Trans. Neural Syst. Rehabil. Eng.* **19**, 411–419 (2011).
36. Clites, T. R., Shepherd, M. K., Ingraham, K. A. & Rouse, E. J. Patient Preference in the Selection of Prosthetic Joint Stiffness. in *2020 8th IEEE RAS/EMBS International Conference for Biomedical Robotics and Biomechatronics (BioRob)* 1073–1079 (2020). doi:10.1109/BioRob49111.2020.9224405.
37. Kim, M., Lyness, H., Chen, T. & Collins, S. H. The Effects of Prosthesis Inversion/Eversion Stiffness on Balance-Related Variability During Level Walking: A Pilot Study. *J. Biomech. Eng.* **142**, (2020).
38. Reimann, H., Fettrow, T., Thompson, E. D. & Jeka, J. J. Neural Control of Balance During Walking. *Front. Physiol.* **9**, 1271 (2018).
39. Gates, D. H., Scott, S. J., Wilken, J. M. & Dingwell, J. B. Frontal plane dynamic margins of stability in individuals with and without transtibial amputation walking on a loose rock surface. *Gait Posture* **38**, 570–575 (2013).
40. Reimann, H. *et al.* Complementary mechanisms for upright balance during walking. *PLOS ONE* **12**, e0172215 (2017).
41. Velzen, J. M. van, Houdijk, H., Polomski, W. & Bennekom, C. A. M. van. Usability of gait analysis in the alignment of trans-tibial prostheses: A clinical study. *Prosthet. Orthot. Int.* **29**, 255–267 (2005).
42. van Hal, E. S., Curtze, C., Postema, K., Hijmans, J. M. & Otten, E. Frontal plane roll-over analysis of prosthetic feet. *J. Biomech.* **125**, 110610 (2021).
43. Segal, A. D. & Klute, G. K. Lower-limb amputee recovery response to an imposed error in mediolateral foot placement. *J. Biomech.* **47**, 2911–2918 (2014).
44. Segal, A. D., Shofer, J. B. & Klute, G. K. Lower-limb amputee ankle and hip kinetic response to an imposed error in mediolateral foot placement. *J. Biomech.* **48**, 3982–3988 (2015).
45. Ramstrand, N. & Nilsson, K.-Å. A Comparison of Foot Placement Strategies of Transtibial Amputees and Able-Bodied Subjects During Stair Ambulation. *Prosthet. Orthot. Int.* **33**, 348–355 (2009).

46. Boone, D. A. *et al.* Influence of malalignment on socket reaction moments during gait in amputees with transtibial prostheses. *Gait Posture* **37**, 620–626 (2013).
47. Royer, T. D. & Wasilewski, C. A. Hip and knee frontal plane moments in persons with unilateral, trans-tibial amputation. *Gait Posture* **23**, 303–306 (2006).
48. Morgenroth, D. C. *et al.* The effect of prosthetic foot push-off on mechanical loading associated with knee osteoarthritis in lower extremity amputees. *Gait Posture* **34**, 502–507 (2011).
49. Jin, L., Adamczyk, P. G., Roland, M. & Hahn, M. E. The Effect of High- and Low-Damping Prosthetic Foot Structures on Knee Loading in the Uninvolved Limb Across Different Walking Speeds. *J. Appl. Biomech.* **32**, 233–240 (2016).
50. Doyle, S. S., Lemaire, E. D., Nantel, J. & Sinitski, E. H. The effect of surface inclination and limb on knee loading measures in transtibial prosthesis users. *J. NeuroEngineering Rehabil.* **16**, 37 (2019).
51. Rueda, F. M. *et al.* Knee and hip internal moments and upper-body kinematics in the frontal plane in unilateral transtibial amputees. *Gait Posture* **37**, 436–439 (2013).
52. Molina-Rueda, F. *et al.* Thorax, pelvis and hip pattern in the frontal plane during walking in unilateral transtibial amputees: biomechanical analysis. *Braz. J. Phys. Ther.* **18**, 252–258 (2014).
53. Molina-Rueda1, F. *et al.* Joint internal moments in subjects with unilateral transtibial amputation during walking. *J. Orthop. Orthop. Surg.* **2**, (2021).
54. Ventura, J. D., Klute, G. K. & Neptune, R. R. The effects of prosthetic ankle dorsiflexion and energy return on below-knee amputee leg loading. *Clin. Biomech.* **26**, 298–303 (2011).
55. McAndrew Young, P. M., Wilken, J. M. & Dingwell, J. B. Dynamic Margins of Stability During Human Walking in Destabilizing Environments. *J. Biomech.* **45**, 1053–1059 (2012).
56. Beltran, E. J., Dingwell, J. B. & Wilken, J. M. Margins of stability in young adults with traumatic transtibial amputation walking in destabilizing environments. *J. Biomech.* **47**, 1138–1143 (2014).
57. Sheehan, R. C., Beltran, E. J., Dingwell, J. B. & Wilken, J. M. Mediolateral angular momentum changes in persons with amputation during perturbed walking. *Gait Posture* **41**, 795–800 (2015).
58. Miller, S. E. Balance recovery mechanisms used by below-knee amputees following mediolateral perturbations. (2017). doi:10.15781/T20V89V4K.
59. Shell, C. E., Segal, A. D., Klute, G. K. & Neptune, R. R. The effects of prosthetic foot stiffness on transtibial amputee walking mechanics and balance control during turning. *Clin. Biomech.* **49**, 56–63 (2017).
60. Vitali, R. V., McGinnis, R. S. & Perkins, N. C. Robust Error-State Kalman Filter for Estimating IMU Orientation. *IEEE Sens. J.* **21**, 3561–3569 (2021).
61. Washabaugh, E. P., Kalyanaraman, T., Adamczyk, P. G., Claflin, E. S. & Krishnan, C. Validity and repeatability of inertial measurement units for measuring gait parameters. *Gait Posture* **55**, 87–93 (2017).
62. Li, Q., Young, M., Naing, V. & Donelan, J. M. Walking speed and slope estimation using shank-mounted inertial measurement units. in *2009 IEEE International Conference on Rehabilitation Robotics* 839–844 (2009). doi:10.1109/ICORR.2009.5209598.
63. Rebula, J. R., Ojeda, L. V., Adamczyk, P. G. & Kuo, A. D. Measurement of foot placement and its variability with inertial sensors. *Gait Posture* **38**, 974–980 (2013).
64. Kitagawa, N. & Ogihara, N. Estimation of foot trajectory during human walking by a wearable inertial measurement unit mounted to the foot. *Gait Posture* **45**, 110–114 (2016).
65. Ojeda, L. V., Rebula, J. R., Kuo, A. D. & Adamczyk, P. G. Influence of contextual task constraints on preferred stride parameters and their variabilities during human walking. *Med. Eng. Phys.* **37**, 929–936 (2015).
66. Gao, F., Liu, G., Liang, F. & Liao, W.-H. IMU-Based Locomotion Mode Identification for Transtibial Prostheses, Orthoses, and Exoskeletons. *IEEE Trans. Neural Syst. Rehabil. Eng.* **28**, 1334–1343 (2020).
67. Sup, F., Varol, H. A. & Goldfarb, M. Upslope Walking With a Powered Knee and Ankle Prosthesis: Initial Results With an Amputee Subject. *IEEE Trans. Neural Syst. Rehabil. Eng.* **19**, 71–78 (2011).

68. Best, T. K., Embry, K. R., Rouse, E. J. & Gregg, R. D. Phase-Variable Control of a Powered Knee-Ankle Prosthesis over Continuously Varying Speeds and Inclines. 8.
69. Takahashi, K. Z., Kepple, T. M. & Stanhope, S. J. A unified deformable (UD) segment model for quantifying total power of anatomical and prosthetic below-knee structures during stance in gait. *J. Biomech.* **45**, 2662–2667 (2012).
70. Torburn, L., Perry, J., Ayyappa, E. & Shanfield, S. L. Below-knee amputee gait with dynamic elastic response prosthetic feet: a pilot study. *J. Rehabil. Res. Dev.* **27**, 369–384 (1990).
71. Schwartz, M. H. & Rozumalski, A. A new method for estimating joint parameters from motion data. *J. Biomech.* **38**, 107–116 (2005).
72. Morgenroth, D. C. *A Prosthetic Foot Emulator to Optimize Prescription of Prosthetic Feet in Veterans and Service Members with Leg Amputations*. https://apps.dtic.mil/docs/citations/AD1046252 (2017).
73. Darter, B. J. & Wilken, J. M. Energetic consequences of using a prosthesis with adaptive ankle motion during slope walking in persons with a transtibial amputation. *Prosthet. Orthot. Int.* **38**, 5–11 (2014).
74. De Asha, A. R., Munjal, R., Kulkarni, J. & Buckley, J. G. Walking speed related joint kinetic alterations in trans-tibial amputees: impact of hydraulic 'ankle' damping. *J. NeuroEngineering Rehabil.* **10**, 107 (2013).
75. Li, T., Wang, L., Yi, J., Li, Q. & Liu, T. Reconstructing Walking Dynamics from Two Shank-Mounted Inertial Measurement Units (IMUs). *IEEEASME Trans. Mechatron.* 1–1 (2021) doi:10.1109/TMECH.2021.3051724.
76. Xu, D. & Wang, Q. On-board Training Strategy for IMU-Based Real-Time Locomotion Recognition of Transtibial Amputees With Robotic Prostheses. *Front. Neurorobotics* **14**, 47 (2020).
77. Hansen, A. H., Sam, M. & Childress, D. S. The Effective Foot Length Ratio: A Potential Tool for Characterization and Evaluation of Prosthetic Feet. *J. Prosthet. Orthot.* **16**, 41–45 (2004).
78. McGeehan, M. A., Adamczyk, P. G., Nichols, K. M. & Hahn, M. E. A Reduced-Order Computational Model of a Semi-Active Variable-Stiffness Foot Prosthesis. *J. Biomech. Eng.* **143**, (2021).
79. McGeehan, M. A., Adamczyk, P. G., Nichols, K. M. & Hahn, M. E. A Computational Gait Model With a Below-Knee Amputation and a Semi-Active Variable-Stiffness Foot Prosthesis. *J. Biomech. Eng.* **143**, (2021).
80. Congressionally Directed Medical Research Programs (CDMRP) Search Awards. https://cdmrp.army.mil/search.aspx?LOG_NO=DM190827.
81. Paulich, M., Schepers, M., Rudigkeit, N. & Bellusci, G. *Xsens MTw Awinda: Miniature Wireless Inertial-Magnetic Motion Tracker for Highly Accurate 3D Kinematic Applications*. (2018). doi:10.13140/RG.2.2.23576.49929.
82. Stolyarov, R., Carney, M. & Herr, H. Accurate Heuristic Terrain Prediction in Powered Lower-Limb Prostheses Using Onboard Sensors. *IEEE Trans. Biomed. Eng.* **68**, 384–392 (2021).
83. Bhakta, K., Camargo, J., Donovan, L., Herrin, K. & Young, A. Machine Learning Model Comparisons of User Independent amp; Dependent Intent Recognition Systems for Powered Prostheses. *IEEE Robot. Autom. Lett.* **5**, 5393–5400 (2020).